

ELIMINATION OF THE QRPA SPURIOUS MODES

A. Repko¹, J. Kvasil², V.O. Nesterenko^{3,4,5}

¹ *Institute of Physics, Slovak Academy of Sciences, 84511, Bratislava, Slovakia**

² *Institute of Particle and Nuclear Physics, Charles University, CZ-18000, Praha 8, Czech Republic[†]*

³ *Laboratory of Theoretical Physics, Joint Institute for Nuclear Research, Dubna, Moscow region, 141980, Russia*

⁴ *State University "Dubna", Dubna, Moscow Region, 141980, Russia and*

⁵ *Moscow Institute of Physics and Technology, Dolgoprudny, Moscow region, 141701, Russia[‡]*

(Dated: September 7, 2018)

We introduce an universal method for elimination of the spurious modes from the intrinsic nuclear excitations described in the framework of the Quasiparticle-Random-Phase-Approximation (QRPA). The method is suitable for any type of spurious admixtures. The efficiency of the method is demonstrated for the case of the Skyrme QRPA applied to the axially deformed ¹⁵⁴Sm. Extraction of the spurious admixtures related with violation of the translational invariance (isovector E1 and isoscalar toroidal and compression E1 excitations), rotational invariance (E2(K=1) excitations), and with pairing-induced non-conservation of the particle number (E2(K=0) and E0 excitations) is considered in detail.

PACS numbers: 24.30.Cz, 21.60.Jz, 13.40.-f, 27.80.+w

I. INTRODUCTION AND MOTIVATION

Theoretical analysis of intrinsic nuclear excitations is often complicated by the presence of spurious modes [1–4]. These modes appear in the intrinsic spectra if some symmetries (translational, rotational) and corresponding conservation laws (for the total momentum \vec{P} and angular momentum \vec{J}) are violated by the intrinsic Hamiltonian. The spurious modes of this kind represent the motion of the whole nucleus (translation, rotation) in the laboratory frame. They are obviously beyond the intrinsic nuclear dynamics and so have to be removed from the intrinsic spectra. Another particular case is the pairing-induced non-conservation of the proton and neutron numbers, when the nuclear wave function is contaminated by admixtures from neighbouring nuclei.

Usually, theoretical spectra acquire spurious admixtures (SA) at the stage of calculation of the static mean field and pairing contribution. There are many ways to suppress SA in nuclear wave functions and electromagnetic responses (transition matrix elements). In E1 isovector responses, the SA caused by center-of-mass motion are usually removed using the proper effective charges [3]. The extraction of the averaged center-of-mass energy from the energy functionals is also in practice, see e.g. [5, 6]. In the second-order E1 toroidal and compression isoscalar responses, the SA are removed through the corrections in the transition operators, requiring the nuclear center-of-mass to be in rest [7–9]. There is also a diversity of projection techniques to refine the states from SA, e.g. [3, 6, 10–14].

Random Phase Approximation (RPA) or its quasipar-

ticle version (QRPA) are now widely used for the self-consistent description of giant resonances and low-energy states in spherical and deformed nuclei, see e.g. [5, 6, 9–20]. As was first shown by Thouless [21, 22], RPA has a principle ability to separate exactly spurious and physical states. In this method, the spurious mode can be built as the RPA eigenstate with the zero energy, which guaranties the orthogonality of the spurious and physical states. Various aspects of this RPA/QRPA feature are described in detail elsewhere, see e.g. [1–4, 23].

This RPA/QRPA advantage was used in early studies within schematic models where violated symmetries were restored by the proper choice of the residual interaction compensating the contamination of the mean field [24]. However this scheme is not relevant for the modern self-consistent QRPA methods (Skyrme, Gogny, relativistic) where the QRPA residual interaction is already fully determined by the initial density functional, see reviews [5, 15]. Another technique, also not self-consistent, offers additional terms in the QRPA residual interaction to shift the spurious modes outside the energy region of interest [25, 26].

As mentioned above, in fully self-consistent RPA/QRPA models with a complete configuration space, the spurious modes have to be entirely located at zero-energy eigenstates. However, even in modern self-consistent QRPA calculations, the extraction of SA is usually not complete, see e.g. [5, 16]. Due to a limited size of configuration space and a numerical inaccuracy, we are almost never able to put the spurious state exactly to the zero energy. Instead, its energy is usually a small positive value. Then the exact spurious mode is not orthogonal to physical states and contaminates them, at least neighboring ones. So the problem of SA persists even in modern self-consistent models.

In the present paper, we propose a simple and universal method for elimination of SA from QRPA states and electromagnetic responses. The method allows to extract

*Electronic address: anton@a-repko.sk

[†]Electronic address: kvasil@ipnp.troja.mff.cuni.cz

[‡]Electronic address: nester@theor.jinr.ru

arbitrary (related with different symmetries) SA in the framework of one and the same scheme. We partly use the idea [10, 11] to refine the physical states requiring their orthogonality to the spurious mode. However, in our study, this idea is realized in a general way using basic QRPA properties. It becomes possible to remove SA from QRPA wave functions and, what is more practicable, directly from electromagnetic responses. Moreover, our amendments to the responses reproduce familiar effective charges and corrections [3, 8]. The method can be applied to both spherical and deformed nuclei. We present the formalism and numerical illustrations obtained within the self-consistent Skyrme QRPA. The main relevant cases are considered: violation of the translational and rotational invariance and pairing-induced non-conservation of the particle number.

The paper is organized as follows. In Section II, the QRPA background and detailed description of the method are presented. In Section III, we demonstrate and discuss examples of SA elimination from E1, E2, and M1 excitations in the axially deformed nucleus ^{154}Sm . In Sec. IV, the conclusions are done.

II. THEORETICAL FRAMEWORK

A. QRPA equations

In this subsection, we sketch the basics of QRPA formalism [3] used below in derivations and analysis. We consider even-even axially-deformed nuclei with the states characterized by quantum numbers K^π where K is the projection of the total moment to the symmetry axis z and π is the space parity. For the nuclear multipole $\lambda\mu$ interaction, we have $K = \mu$ and $\pi = (-1)^\lambda$ for electric, or $\pi = (-1)^{\lambda+1}$ for magnetic modes.

The intrinsic body-fixed Hamiltonian reads

$$\hat{H}_{\text{intr}} = \hat{H}_{\text{BCS}} + \hat{V}_{\text{res}} \quad (1)$$

where \hat{H}_{BCS} describes mean field and pairing, \hat{V}_{res} is the residual interaction.

One-phonon QRPA eigenstates $Q_\nu^\dagger|0\rangle$ (with $|0\rangle$ being the QRPA vacuum) are described by the phonon creation operator

$$Q_\nu^\dagger = \sum_{i>j} (X_{ij}^{(\nu)} \alpha_i^\dagger \alpha_j^\dagger - Y_{ij}^{(\nu)} \alpha_{\bar{j}} \alpha_{\bar{i}}) \quad (2)$$

defined as a superposition of \mathcal{N} two-quasiparticle (2qp) ij -excitations with quantum numbers μ^π . The pairs ij with $K_i + K_j = \mu$ and $i\bar{j}$ with $K_i - K_j = \mu$ are used. The condition $i > j$ means that we involve configurations with $K_i > K_j > 0$, and, if it is allowed by selection rules, also $K_i = K_j > 0$ (with a separate criterion on ordering; and with specific symmetrization in the case of $\mu = 0$); ν numerates the phonons with given μ^π ; $X_{ij}^{(\nu)}$ and $Y_{ij}^{(\nu)}$ are forward and backward 2qp amplitudes; $|\bar{i}\rangle = \mathcal{T}|i\rangle$ are

time-reversed states. The time-reversed counterpart of (2) reads

$$Q_{\bar{\nu}}^\dagger = \sum_{i>j} (X_{ij}^{(\nu)*} \alpha_{\bar{i}}^\dagger \alpha_{\bar{j}}^\dagger - Y_{ij}^{(\nu)*} \alpha_j \alpha_i). \quad (3)$$

Amplitudes $X_{ij}^{(\nu)}$ and $Y_{ij}^{(\nu)}$ and phonon energies $\hbar\omega_\nu$ are obtained from QRPA equations of motion

$$[\hat{H}_{\text{intr}}, Q_\nu^\dagger] = \hbar\omega_\nu Q_\nu^\dagger, \quad (4a)$$

$$[\hat{H}_{\text{intr}}, Q_\nu] = -\hbar\omega_\nu Q_\nu, \quad (4b)$$

$$[Q_\nu, Q_{\nu'}^\dagger] = \delta_{\nu\nu'}. \quad (4c)$$

In the matrix form, these equations read [3]

$$\begin{pmatrix} A & B \\ B & A \end{pmatrix} \begin{pmatrix} X^{(\nu)} \\ Y^{(\nu)} \end{pmatrix} = \hbar\omega_\nu \begin{pmatrix} X^{(\nu)} \\ -Y^{(\nu)} \end{pmatrix}. \quad (5)$$

They include real matrices A and B :

$$A_{ij\ i'j'} \equiv (E_i + E_j) \delta_{ij\ i'j'} + \langle BCS | [\alpha_j \alpha_i, [\hat{V}_{\text{res}}, \alpha_{i'}^\dagger \alpha_{j'}^\dagger]] | BCS \rangle, \quad (6a)$$

$$B_{ij\ i'j'} \equiv -\langle BCS | [\alpha_j \alpha_i, [\hat{V}_{\text{res}}, \alpha_{\bar{j}'} \alpha_{\bar{i}'}]] | BCS \rangle \quad (6b)$$

and one-column matrices

$$X^{(\nu)} \equiv \begin{pmatrix} \vdots \\ X_{ij}^{(\nu)} \\ \vdots \end{pmatrix} \quad Y^{(\nu)} \equiv \begin{pmatrix} \vdots \\ Y_{ij}^{(\nu)} \\ \vdots \end{pmatrix} \quad ij = 1, \dots, \mathcal{N}. \quad (7)$$

According to our time-reversal convention for one-body operators \hat{A} ,

$$\mathcal{T}^{-1} \hat{A} \mathcal{T} = \gamma_{\mathcal{T}}^A \hat{A}^\dagger \Rightarrow \langle i | \hat{A} | j \rangle = \gamma_{\mathcal{T}}^A \langle \bar{j} | \hat{A} | \bar{i} \rangle, \quad \langle i | \hat{A} | \bar{j} \rangle = -\gamma_{\mathcal{T}}^A \langle j | \hat{A} | \bar{i} \rangle, \quad (8)$$

we introduce time-even ($\gamma_{\mathcal{T}}^A = +1$) and time-odd ($\gamma_{\mathcal{T}}^A = -1$) operators. Then, instead of the phonon creation and annihilation operators, one may define the generalized time-even coordinate and time-odd momentum operators

$$\hat{\mathcal{X}}_\nu = \sum_{i>j} \mathcal{X}_{ij}^{(\nu)} (\alpha_i^\dagger \alpha_j^\dagger + \alpha_{\bar{j}} \alpha_{\bar{i}}), \quad (9a)$$

$$\hat{\mathcal{P}}_\nu = \sum_{i>j} \mathcal{P}_{ij}^{(\nu)} (\alpha_i^\dagger \alpha_j^\dagger - \alpha_{\bar{j}} \alpha_{\bar{i}}). \quad (9b)$$

Following (8), their time-reversed conjugates are

$$\hat{\mathcal{X}}_{\bar{\nu}} \equiv \hat{\mathcal{X}}_\nu^\dagger, \quad \hat{\mathcal{P}}_{\bar{\nu}} \equiv -\hat{\mathcal{P}}_\nu^\dagger, \quad (10a)$$

$$\mathcal{X}_{i\bar{j}}^{(\bar{\nu})} = \mathcal{X}_{ij}^{(\nu)*}, \quad \mathcal{P}_{i\bar{j}}^{(\bar{\nu})} = \mathcal{P}_{ij}^{(\nu)*}. \quad (10b)$$

The new operators $\hat{\mathcal{X}}_\nu$ and $\hat{\mathcal{P}}_\nu$ are related to the phonon operators (2)-(3) as

$$\hat{\mathcal{X}}_\nu = \sqrt{\frac{\hbar}{M_\nu \omega_\nu}} \frac{1}{\sqrt{2}} (Q_{\bar{\nu}} + Q_\nu^\dagger), \quad (11a)$$

$$\hat{\mathcal{P}}_\nu = \frac{\hbar}{i} \sqrt{\frac{M_\nu \omega_\nu}{\hbar}} \frac{1}{\sqrt{2}} (Q_{\bar{\nu}} - Q_\nu^\dagger) \quad (11b)$$

and vice versa,

$$Q_\nu^\dagger = \sqrt{\frac{M_\nu \omega_\nu}{2\hbar}} \hat{\mathcal{X}}_\nu - \frac{i}{\sqrt{2\hbar M_\nu \omega_\nu}} \hat{\mathcal{P}}_\nu, \quad (12a)$$

$$Q_{\bar{\nu}} = \sqrt{\frac{M_\nu \omega_\nu}{2\hbar}} \hat{\mathcal{X}}_\nu + \frac{i}{\sqrt{2\hbar M_\nu \omega_\nu}} \hat{\mathcal{P}}_\nu. \quad (12b)$$

The orthonormalization condition is

$$[\hat{\mathcal{X}}_\nu, \hat{\mathcal{P}}_{\nu'}^\dagger] = -2 \sum_{i>j} \mathcal{X}_{ij}^{(\nu)} \mathcal{P}_{ij}^{(\nu')*} = i\hbar \delta_{\nu\nu'}. \quad (13)$$

If $\mathcal{X}_{ij}^{(\nu)}$ is real then $\mathcal{P}_{ij}^{(\nu)}$ is imaginary, and vice versa. Following (11)-(13), the operators $\hat{\mathcal{X}}_\nu$ and $\hat{\mathcal{P}}_\nu$ are defined up to an arbitrary factor M_ν which cannot be fixed by the normalization condition.

The QRPA equations (4) can be expressed in terms of $\hat{\mathcal{X}}_\nu$ and $\hat{\mathcal{P}}_\nu$ as

$$[\hat{H}_{intr}, \hat{\mathcal{P}}_\nu] = i\hbar M_\nu \omega_\nu^2 \hat{\mathcal{X}}_\nu, \quad (14a)$$

$$[\hat{H}_{intr}, \hat{\mathcal{X}}_\nu] = -\frac{i\hbar}{M_\nu} \hat{\mathcal{P}}_\nu, \quad (14b)$$

$$[\hat{\mathcal{X}}_\nu, \hat{\mathcal{P}}_{\nu'}^\dagger] = i\hbar \delta_{\nu\nu'}, \quad (14c)$$

or, in the matrix form, as

$$\begin{pmatrix} A & B \\ B & A \end{pmatrix} \begin{pmatrix} \mathcal{P}^{(\nu)} \\ \mathcal{P}^{(\nu)} \end{pmatrix} = i\hbar M_\nu \omega_\nu^2 \begin{pmatrix} \mathcal{X}^{(\nu)} \\ \mathcal{X}^{(\nu)} \end{pmatrix}, \quad (15a)$$

$$\begin{pmatrix} A & B \\ B & A \end{pmatrix} \begin{pmatrix} \mathcal{X}^{(\nu)} \\ -\mathcal{X}^{(\nu)} \end{pmatrix} = \frac{\hbar}{i} \frac{1}{M_\nu} \begin{pmatrix} \mathcal{P}^{(\nu)} \\ -\mathcal{P}^{(\nu)} \end{pmatrix}, \quad (15b)$$

where, in analogy with (7), $\mathcal{X}^{(\nu)}$ and $\mathcal{P}^{(\nu)}$ are one-column matrices for 2qp amplitudes of the generalized coordinates and momenta.

For given K^π , the intrinsic Hamiltonian (1) in terms of $\hat{\mathcal{X}}_\nu$ and $\hat{\mathcal{P}}_\nu$ has the form

$$\hat{H}_{intr} \approx \hat{H}_{QRPA} = \sum_\nu \left(\frac{\hat{\mathcal{P}}_\nu \hat{\mathcal{P}}_\nu^\dagger}{2M_\nu} + \frac{1}{2} M_\nu \omega_\nu^2 \hat{\mathcal{X}}_\nu \hat{\mathcal{X}}_\nu^\dagger \right). \quad (16)$$

This expression shows that arbitrary parameter M_ν can be treated as an inertia (mass) value characterizing each QRPA state.

Note that $\langle \hat{\mathcal{X}}, \hat{\mathcal{P}} \rangle$ -presentation can be fruitful for construction of modern self-consistent QRPA versions based on the functionals with time-even and time-odd densities and currents [27], see particular cases of Skyrme QRPA in [28, 29].

B. Extraction of spurious admixtures

The invariance of the Hamiltonian \hat{H}_{intr} under translation or rotation of the whole nucleus leads to the conservation condition

$$[\hat{H}_{intr}, \hat{P}] = 0 \quad (17)$$

where \hat{P} is the corresponding time-odd transformation generator. The motion of the whole nucleus contaminates the intrinsic nuclear excitations and leads to SA which have to be extracted from the intrinsic spectra. For the translation, the generator \hat{P} is the linear momentum operator of the whole nucleus. In axial deformed nuclei, the center-of-mass translation contaminates the intrinsic $K^\pi = 0^-$ and 1^- states. For the rotation, \hat{P} is the total angular momentum operator. The rotation pollutes intrinsic $K^\pi = 1^+$ states.

As shown by Thouless [21, 22], just $\langle \hat{\mathcal{X}}, \hat{\mathcal{P}} \rangle$ -presentation of QRPA is suitable for the treatment of spurious modes. Indeed, it is easy to see that QRPA equation (14) reproduces the condition (17) if $\omega_0 = 0$ and generator \hat{P} is identified with the QRPA generalized momentum $\hat{\mathcal{P}}_0$. Then the Hamiltonian (16) recasts to

$$\hat{H}_{QRPA} = \frac{\hat{\mathcal{P}}_0 \hat{\mathcal{P}}_0^\dagger}{2M_0} + \sum_{\nu \neq 0} \left(\frac{\hat{\mathcal{P}}_\nu \hat{\mathcal{P}}_\nu^\dagger}{2M_\nu} + \frac{1}{2} M_\nu \omega_\nu^2 \hat{\mathcal{X}}_\nu \hat{\mathcal{X}}_\nu^\dagger \right) \quad (18)$$

where the spurious $\nu = 0$ state with $\omega_0 = 0$ yields the first term [3]. The generalized coordinate $\hat{\mathcal{X}}_0$ is obtained from Eq. (14b) for given $\hat{\mathcal{P}}_0$. Note that $\hat{\mathcal{X}}_0$ is absent in (18). The spaces $\{\hat{\mathcal{X}}_0, \hat{\mathcal{P}}_0, \hat{\mathcal{X}}_{\nu>0}, \hat{\mathcal{P}}_{\nu>0}\}$ and $\{\hat{\mathcal{X}}_0, \hat{\mathcal{P}}_0, Q_{\nu>0}^\dagger, Q_{\nu>0}\}$ constitute the complete sets of QRPA states. The condition $\omega_0 = 0$ obviously hampers the construction of well-normalized spurious (s) phonon operator

$$Q_s^\dagger \equiv x_s \hat{\mathcal{X}}_0 - \frac{i}{2\hbar x_s} \hat{\mathcal{P}}_0 \quad (19)$$

with $x_s = \sqrt{M_0 \omega_0 / (2\hbar)}$. So the *exact* spurious eigenstate can be defined in terms of $\hat{\mathcal{X}}_0$ and $\hat{\mathcal{P}}_0$ but not in the phonon representation.

In addition to (17), one may also consider the conservation law for the particle number,

$$[\hat{H}_{intr}, \hat{N}_q] = 0, \quad (20)$$

where \hat{N}_q is the time-even particle-number operator for protons ($q = p$) or neutrons ($q = n$). Violation of this law results in spurious admixtures in $K^\pi = 0^+$ states. The condition (20) is held by the QRPA equation (14b) if a) \hat{N} is identified with the QRPA generalized coordinate $\hat{\mathcal{X}}_0$ and b) we apply $M_0 \rightarrow +\infty$ and $\omega_0 \rightarrow 0$ while keeping $M_0 \omega_0^2$ finite (though the requirement b) can hardly be realized in practice).

As mentioned in the Introduction, in self-consistent QRPA calculations we are almost never able to put the energy of the first eigenstate precisely to zero. Even large 2qp basis is usually not enough to get $\omega_0 = 0$. As a result, the conservation laws (17) and (20) are not held precisely and the spurious mode, though being mainly concentrated in the lowest $\nu = 0$ state, still contaminates the neighbouring physical states with $\nu > 0$. Then the spurious mode and physical states are not exactly orthogonal. However, at $\omega_0 > 0$, the primarily spurious state (19) can be normalized.

Our method for elimination of SA from QRPA physical states just addresses the case with $\omega_0 > 0$. Let's assume the initial set of QRPA states $|\nu'\rangle \equiv Q_{\nu'}^\dagger|0\rangle$ where the first $\nu' = 0$ state (19) is quasi-spurious with $\omega_0 > 0$. This set corresponds to the Hamiltonian (16).¹ The name "quasi-spurious" means that the state is almost pure spurious and its energy ω_0 is very small positive value. This is a good approximation to the exact spurious state. What is important, the quasi-spurious state with $\omega_0 > 0$ can be normalized and phonon presentation remains applicable. In what follows, we will approximate the true spurious state by the quasi-spurious state $|s\rangle \approx Q_{\nu'=0}^\dagger|0\rangle$. Since $\omega_0 > 0$, we actually have two quasi-spurious states, $|s\rangle$ and $|\tilde{s}\rangle$. Below we consider only $|s\rangle$ since, due to the axial symmetry, all the results for $|s\rangle$ are valid for $|\tilde{s}\rangle$. The state $|s\rangle$ is supposed to be normalized in accordance to Eq. (13):

$$[\hat{\mathcal{X}}_0, \hat{\mathcal{P}}_0^\dagger] = i\hbar. \quad (21)$$

The quasi-spurious state $|s\rangle$ apparently covers both the case (17) with $\hat{P} \sim \hat{\mathcal{P}}_0$ and the case (20) with $\hat{N} \sim \hat{\mathcal{X}}_0$. In the phonon presentation, $|s\rangle$ has the form (19).

Now let's suppose that we have the set of QRPA self-consistent solutions $|\nu\rangle = Q_\nu^\dagger|\tilde{0}\rangle$ (with the vacuum $|\tilde{0}\rangle$ defined by $Q_\nu|\tilde{0}\rangle$) contaminated by SA. Our goal is to refine the states $|\nu\rangle$ from SA. This can be done requiring orthogonality of the refined states to the spurious mode (in our case to the quasi-spurious state $|s\rangle$). After the orthonormalization, the refined states should be close to the states $|\nu'\rangle$ mentioned above. So, in what follows, we use for the refined states the notation $|\nu'\rangle$ (and $|0\rangle$ for their vacuum). Then condition of the orthogonality of the refined ($\nu' > 0$) states to the spurious mode reads

$$\langle\nu'|s\rangle = \langle 0|[Q_{\nu'}, Q_s^\dagger]|0\rangle = 0 \quad (22)$$

The phonon operator for the refined state $|\nu'\rangle = Q_{\nu'}^\dagger|0\rangle$ is searched in the form

$$Q_{\nu'}^\dagger = Q_\nu^\dagger - \alpha_\nu \hat{\mathcal{P}}_0 - \beta_\nu \hat{\mathcal{X}}_0. \quad (23)$$

This prescription reminds the projection methods used in some previous studies (see e.g. [10, 11, 13]) for particular spurious modes. However here we use a more general expression (19) for the spurious state, including both $\hat{\mathcal{X}}_0$ and $\hat{\mathcal{P}}_0$ operators (as compared to [10, 13], where the translational spurious state is $\hat{\mathcal{X}}_0|0\rangle$). As shown below, our way allows to derive a more general scheme for elimination of SA.

The condition (22) gives

$$\alpha_\nu = \left[\frac{\langle 0|[Q_\nu, \hat{\mathcal{X}}_0]|0\rangle}{\langle 0|[\hat{\mathcal{P}}_0^\dagger, \hat{\mathcal{X}}_0]|0\rangle} \right]^*, \beta_\nu = \left[\frac{\langle 0|[Q_\nu, \hat{\mathcal{P}}_0]|0\rangle}{\langle 0|[\hat{\mathcal{X}}_0^\dagger, \hat{\mathcal{P}}_0]|0\rangle} \right]^* \quad (24)$$

or, using (21),

$$\alpha_\nu = \frac{1}{i\hbar} \langle 0|[Q_\nu, \hat{\mathcal{X}}_0]|0\rangle^*, \beta_\nu = \frac{i}{\hbar} \langle 0|[Q_\nu, \hat{\mathcal{P}}_0]|0\rangle^*. \quad (25)$$

It is easy to check that

$$\langle 0|[Q_{\nu'}, \hat{\mathcal{X}}_0]|0\rangle = \langle 0|[Q_{\nu'}, \hat{\mathcal{P}}_0]|0\rangle = 0 \quad (26)$$

i.e., within the quasiboson approximation, the refined physical states are indeed orthogonal to the generators \mathcal{P}_0 and \mathcal{X}_0 and so to the spurious state (19). In this derivation, we use the feature that the average commutator $\langle 0|[\hat{A}, \hat{B}]|0\rangle$ vanishes if operators \hat{A} and \hat{B} have the same time-parity in the sense (8).

Note that result (26) does not depend on the concrete values of x_s , M_ν and ω_0 . For determination of α_ν and β_ν , we should know the symmetry operator and its conjugate, i.e. $\hat{\mathcal{P}}_0$ and $\hat{\mathcal{X}}_0$. These operators are given below in Sec. III for all the cases of interest.

The above scheme allows to refine QRPA states. However in practice we often need a direct refinement of the transition matrix elements and responses. As shown below, this can be also done within our approach. Let's consider matrix element of one-body transition operator \hat{T} between the physical refined state $|\nu'\rangle$ and the RPA vacuum reads

$$\begin{aligned} \langle\nu'|\hat{T}|0\rangle &= \langle\nu|[Q_\nu, \hat{T}]|0\rangle \\ &\quad - \alpha_\nu^* \langle 0|[\hat{\mathcal{P}}_0^\dagger, \hat{T}]|0\rangle - \beta_\nu^* \langle 0|[\hat{\mathcal{X}}_0^\dagger, \hat{T}]|0\rangle. \end{aligned} \quad (27)$$

Depending on time-parity of \hat{T} , only the second or the third term in (27) is non-zero.

For instance, matrix elements of the time-even operator $\hat{T}_q = \sum_{j \in q} t_q(\vec{r}_j)$ ($q = \text{neut, prot}$) are given by the second term in (27),

$$\begin{aligned} \langle\nu'|\hat{T}_q|0\rangle &= \langle 0|[Q_\nu, \hat{T}_q]|0\rangle \\ &\quad - \frac{\langle 0|[Q_\nu, \hat{\mathcal{X}}_0]|0\rangle}{\langle 0|[Q_s, \hat{\mathcal{X}}_0]|0\rangle} \langle 0|[Q_s, \hat{T}_q]|0\rangle = \\ &= \int d^3r \delta\rho_{\nu; q}(\vec{r}) t_q(\vec{r}) - y_\nu \int d^3r \delta\rho_{s; q}(\vec{r}) t_q(\vec{r}) \end{aligned} \quad (28)$$

taking the freedom to replace $\hat{\mathcal{P}}_0^\dagger \mapsto \hat{Q}_s$; and defining

$$y_\nu = \frac{\langle 0|[Q_\nu, \hat{\mathcal{X}}_0]|0\rangle}{\langle 0|[Q_s, \hat{\mathcal{X}}_0]|0\rangle} = \frac{\int d^3r \delta\rho_\nu(\vec{r}) \mathcal{X}_0(\vec{r})}{\int d^3r \delta\rho_s(\vec{r}) \mathcal{X}_0(\vec{r})} \quad (29)$$

with the transition densities

$$\begin{aligned} \delta\rho_\nu(\vec{r}) &\equiv \sum_{q=n,p} \delta\rho_{\nu; q}(\vec{r}) = \\ &= \sum_{q=n,p} \langle 0|[Q_\nu, \hat{\rho}_q(\vec{r})]|0\rangle \end{aligned} \quad (30)$$

$$\delta\rho_s(\vec{r}) \equiv \sum_{q=n,p} \langle 0|[Q_s, \hat{\rho}_q(\vec{r})]|0\rangle. \quad (31)$$

$\mathcal{X}_0 = \sum_{j=1}^A \mathcal{X}_0(\vec{r}_j)$ in (29) is the coordinate representation of the operator $\hat{\mathcal{X}}_0$, which is time-even, same as the operator of density in (31), $\hat{\rho}_q(\vec{r})$; so only the \mathcal{P}_0 -part of spurious phonon Q_s (19) works in this case.

Similarly, matrix elements of a time-odd transition operator $\hat{T}_q = \sum_{j \in q} t_q(\vec{r}_j)$ (with $\hat{T}^{-1} \hat{T}_q \hat{T} = -\hat{T}_q^\dagger$), between the physical non-spurious states $|\nu'\rangle$ and the RPA vacuum is given by the third term in (27),

$$\langle \nu' | \hat{T}_q | 0 \rangle = \langle \nu | \hat{T}_q | 0 \rangle - z_\nu \langle 0 | [\hat{\mathcal{X}}_0^\dagger, \hat{T}_q] | 0 \rangle \quad (32)$$

where

$$z_\nu = \frac{\langle 0 | [Q_\nu, \hat{\mathcal{P}}_0] | 0 \rangle}{\langle 0 | [\hat{\mathcal{X}}_0^\dagger, \hat{\mathcal{P}}_0] | 0 \rangle} \quad (33)$$

The expressions (32) and (33) can be used e.g. for the calculation of the transition current $\delta \vec{j}_{\nu', q}(\vec{r}) \equiv \langle \nu' | \hat{j}_q(\vec{r}) | 0 \rangle$ which participates in the matrix elements of transition operators depending on the nucleon current $\hat{j}_q(\vec{r})$.

One should realize that in expressions (27), (28) and (32), the factor x_s (see (19)) does not participate explicitly. Nevertheless, both the spurious linear momentum $\hat{\mathcal{P}}_0$ and spurious coordinate $\hat{\mathcal{X}}_0$ are necessary to be known. However, in most cases, only the symmetry-generating operator is known explicitly, namely the $\hat{\mathcal{P}}_0$ operator (or $\hat{\mathcal{X}}_0 = \hat{N}$ in 0^+ case). In such cases, the amplitudes $\mathcal{X}_{ij}^{(0)}$ (or $\mathcal{P}_{ij}^{(0)}$) of corresponding conjugated partner $\hat{\mathcal{X}}_0$ (or $\hat{\mathcal{P}}_0$) should be determined by the inversion from (14b) (or (14a)).

$$\mathcal{X}_{ij}^{(\nu)} = \frac{\hbar}{i} \frac{1}{M_\nu} \sum_{kl=1}^N (A - B)_{ij, kl}^{-1} \mathcal{P}_{kl}^{(\nu)} \quad (34)$$

$$\mathcal{P}_{ij}^{(\nu)} = i \hbar \omega_\nu^2 M_\nu \sum_{kl=1}^N (A + B)_{ij, kl}^{-1} \mathcal{X}_{kl}^{(\nu)}. \quad (35)$$

As was mentioned above, in the case of axially deformed nuclei, the RPA equations (5) or (15) can be solved independently for each value of the angular-momentum projection onto the symmetry axis (μ) and for each value of parity ($\pi = \pm 1$). Then we obtain phonons $Q_{\nu[\mu^\pi]}^\dagger = \sum_{ij} (X_{ij}^{(\nu[\mu^\pi])} \alpha_i^+ \alpha_j^+ - Y_{ij}^{(\nu[\mu^\pi])} \alpha_j \alpha_i)$ with corresponding phonon energies $\hbar \omega_{\nu[\mu^\pi]}$, where we can restrict ourselves to $\mu \geq 0$ for the time-even Hamiltonian. Corresponding angular momentum projections K_i and K_j of the single-quasiparticles α_i^+ and α_j^+ should fulfill the selection rules: $\mu = K_i + K_j$ (or $\mu = K_i - K_j$) and $\pi_\nu = \pi_i \pi_j$ (taking account the ordering mentioned at (2)). In the framework of two-quasiparticle approximation (usually used in the QRPA) all single-particle operators \hat{T} (e.g. the density $\hat{\rho}(\vec{r})$) reduce only to $\alpha_i^+ \alpha_j^+$ and $\alpha_j \alpha_i$ parts ($\hat{T} = \sum_{ij} (\langle ij | \hat{T} | BCS \rangle (\alpha_i^+ \alpha_j^+ + \gamma_T^T \alpha_j \alpha_i)$, where $\langle ij | \hat{T} | BCS \rangle$) are two-quasiparticle matrix elements of the given operator. Then the matrix element $\langle 0 | [Q_\nu, \hat{T}] | 0 \rangle$ for any s.p. transition operator \hat{T} reads

$$\begin{aligned} \langle 0 | [Q_\nu, \hat{T}] | 0 \rangle &= \\ &= \sum_{ij} [X_{ij}^{(\nu[\mu^\pi])^*} + \gamma_T^T Y_{ij}^{(\nu[\mu^\pi])^*}] \langle ij | \hat{T} | BCS \rangle \quad (36) \end{aligned}$$

and similar expression can be written for matrix elements $\langle 0 | [\hat{\mathcal{X}}_0^\dagger, \hat{T}] | 0 \rangle$ and $\langle 0 | [\hat{\mathcal{P}}_0^\dagger, \hat{T}] | 0 \rangle$,

$$\begin{aligned} \langle 0 | [\hat{\mathcal{X}}_0^\dagger, \hat{T}] | 0 \rangle &= \\ &= \begin{cases} 0 & \text{for time-even } \hat{T} \\ \sum_{ij} \langle ij | \hat{\mathcal{X}}_0 | BCS \rangle^* \langle ij | \hat{T} | BCS \rangle = \\ = 2 \sum_{ij} \mathcal{X}_{ij}^{(0)*} \langle ij | \hat{T} | BCS \rangle & \text{for time-odd } \hat{T} \end{cases} \quad (37) \end{aligned}$$

and

$$\begin{aligned} \langle 0 | [\hat{\mathcal{P}}_0^\dagger, \hat{T}] | 0 \rangle &= \\ &= \begin{cases} \sum_{ij} \langle ij | \hat{\mathcal{P}}_0 | BCS \rangle^* \langle ij | \hat{T} | BCS \rangle = \\ = 2 \sum_{ij} \mathcal{P}_{ij}^{(0)*} \langle ij | \hat{T} | BCS \rangle & \text{for time-even } \hat{T} \\ 0 & \text{for time-odd } \hat{T} \end{cases} \quad (38) \end{aligned}$$

because we suppose the spurious linear momentum $\hat{\mathcal{P}}_0$ to be time-odd and spurious coordinate $\hat{\mathcal{X}}_0$ to be time-even.

C. Transition operators and strength functions

In this paper, the method for the elimination of the spuriousity in the QRPA approach described above is demonstrated for the case of $X\lambda\mu$: electromagnetic excitations of different types ($X = E$ (electric), $X = M$ (magnetic)) and different multiplicities λ , with the projection μ . Namely, the spurious elimination for $\mu^\pi = 0^+$ (for $E00$, $E20$ excitations, with the spuriousity related to the particle number operator ($\hat{\mathcal{X}}_0 \equiv \hat{N}$); for $\mu^\pi = 0^-$ (for $E10$, $E10\text{ com}$, $E10\text{ tor}$ excitations) with the spuriousity related to the translation of the nucleus' CoM ($\hat{\mathcal{P}}_0 = -i\hbar \sum_{i=1}^A (\nabla_0)_i - \mu = 0$ component of the nucleus' total linear momentum); for $\mu^\pi = 1^+$ (for $E21$, $M11$ excitations) with the spuriousity mode related to the $\mu = 1$ component of the nucleus' total angular momentum ($\hat{\mathcal{P}}_0 = \hat{J}_{+1}$); and for $\mu^\pi = 1^-$ (for $E11$, $E11\text{ com}$, $E11\text{ tor}$ excitations) with the spuriousity related to $\mu = 1$ component of the nucleus' total linear momentum $\hat{\mathcal{P}}_0 = -i\hbar \sum_{i=1}^A (\nabla_{+1})_i$. The $X\lambda\mu$ transitions are analysed for various isospin transfers $\Delta T = \text{nat}, 0, 1$ ($\Delta T = \text{nat}$ corresponds to the "natural" electromagnetic transition generated by the proton charge and natural nucleon g-factors, $\Delta T = 0$ corresponds to isoscalar transitions, and $\Delta T = 1$ to the isovector transitions). Corresponding transition operators are the following:

- $E00$ transition operator ($\mu^\pi = 0^+$)

$$\hat{\mathcal{M}}_{E00}(\Delta T) = \int d^3r \hat{\rho}_{\Delta T}(\vec{r}) r^2 Y_{00}(\hat{r}), \quad (39)$$

- $E2\mu$ transition operator ($\mu^\pi = 0^+$, $\mu^\pi = 1^+$, $\mu^\pi = 2^+$)

$$\hat{\mathcal{M}}_{E2\mu}(\Delta T) = \int d^3r \hat{\rho}_{\Delta T}(\vec{r}) r^2 Y_{2\mu}(\hat{r}), \quad (40)$$

- $E1\mu$ transition operator ($\mu^\pi = 0^-, \mu^\pi = 1^-$)

$$\hat{\mathcal{M}}_{E1\mu}(\Delta T) = \int d^3r \hat{\rho}_{\Delta T}(\vec{r}) r Y_{1\mu}(\hat{r}), \quad (41)$$

- $E1\mu$ *com* compression transition operator ($\mu^\pi = 0^-, \mu^\pi = 1^-$) (see [9])

$$\hat{\mathcal{M}}_{E1\mu com}(\Delta T) = \frac{1}{10} \int d^3r \hat{\rho}_{\Delta T}(\vec{r}) r^3 Y_{1\mu}(\hat{r}), \quad (42)$$

- $E1\mu$ *tor* toroidal transition operator ($\mu^\pi = 0^-, \mu^\pi = 1^-$) (see [9])

$$\hat{\mathcal{M}}_{E1\mu tor}(\Delta T) = -\frac{i}{2\sqrt{3}} \int d^3r \hat{j}_{nuc; \Delta T}(\vec{r}) \cdot r^2 \left[\vec{Y}_{1\mu}^0(\hat{r}) + \frac{\sqrt{2}}{5} \vec{Y}_{1\mu}^2(\hat{r}) \right] \quad (43)$$

where $\vec{Y}_{JM}^L(\hat{r})$ are vector spherical harmonics (see [30]) and $\hat{j}_{nuc; \Delta T}(\vec{r})$ is the operator of the nucleon current

- and finally, $M1\mu$ long-wave-limit transition operator ($\mu^\pi = 0^+, \mu^\pi = 1^+$) is written as

$$\hat{\mathcal{M}}_{M1\mu}(\Delta T) = \frac{e\hbar}{2mc} \sqrt{\frac{3}{4\pi}} \sum_{j=1}^A [e_{\Delta T}^{(j)} \hat{l}_\mu^{(j)} + g_{\Delta T}^{(j)} \hat{s}_\mu^{(j)}] \quad (44)$$

where m is the nucleon mass, $\hat{l}_\mu^{(j)}$ is the μ -th component of the orbital momentum of the j -th nucleon, $\hat{s}_\mu^{(j)}$ is the μ -th component of the spin of the j -th nucleon, $e_{\Delta T}^{(j)}$ and $g_{\Delta T}^{(j)}$ are the effective charge and the effective gyromagnetic factor of the j -th nucleon for the transition with the isospin change $\Delta T = nat, 0, 1$ (see further). In (39), (40), (41), and (42) the operator $\hat{\rho}_{\Delta T}(\vec{r})$ is the density operator,

$$\hat{\rho}_{\Delta T}(\vec{r}) = \sum_{j=1}^A e_{\Delta T}^{(j)} \delta(\vec{r} - \vec{r}_j) \quad (45)$$

corresponding to the transition with $\Delta T = nat, 0, 1$. The operator of the nuclear current $\hat{j}_{nuc; \Delta T}(\vec{r})$ is given by the sum of the convective and magnetization currents,

$$\hat{j}_{nuc; \Delta T}(\vec{r}) = \hat{j}_{conv; \Delta T}(\vec{r}) + \hat{j}_{magn; \Delta T}(\vec{r}) \quad (46)$$

with

$$\begin{aligned} \hat{j}_{conv; \Delta T}(\vec{r}) &= \sum_{i=1}^A e_{\Delta T}^{(i)} \frac{e}{2mc} [\delta(\vec{r} - \vec{r}_i) \hat{p}_i + \hat{p}_i \delta(\vec{r} - \vec{r}_i)] \\ \hat{j}_{magn; \Delta T}(\vec{r}) &= \vec{\nabla} \times \sum_{i=1}^A \frac{e\hbar}{2mc} g_{\Delta T}^{(i)} \hat{s}_i \delta(\vec{r} - \vec{r}_i) \end{aligned} \quad (47)$$

The effective charges $e_{\Delta T}^{(i)}$ and effective gyromagnetic factors $g_{\Delta T}^{(j)}$ are defined by the change of isospin ΔT as follows

$$\begin{aligned} e_{\Delta T=nat}^{(i)} &= \begin{cases} 1 & \text{for } i \in p \\ 0 & \text{for } i \in n \end{cases}; \quad g_{\Delta T=nat}^{(i)} = \begin{cases} 5.58 \xi & \text{for } i \in p \\ -3.82 \xi & \text{for } i \in n \end{cases} \\ e_{\Delta T=0}^{(i)} &= \begin{cases} \frac{1}{2} & \text{for } i \in p \\ \frac{1}{2} & \text{for } i \in n \end{cases}; \quad g_{\Delta T=0}^{(i)} = \begin{cases} 0.88 \xi & \text{for } i \in p \\ 0.88 \xi & \text{for } i \in n \end{cases} \\ e_{\Delta T=1}^{(i)} &= \begin{cases} \frac{1}{2} & \text{for } i \in p \\ -\frac{1}{2} & \text{for } i \in n \end{cases}; \quad g_{\Delta T=1}^{(i)} = \begin{cases} 4.7 \xi & \text{for } i \in p \\ -4.7 \xi & \text{for } i \in n \end{cases} \end{aligned} \quad (48)$$

where $\xi \approx 0.7$ is the quenching for gyromagnetic factor related to the meson exchange currents in the nucleus (see [31]).

Using the matrix elements of transition operators $\hat{\mathcal{M}}_{X\lambda\mu}(\Delta T)$ (39–44) between the physical non-spurious states $|\nu'\rangle$ and the RPA vacuum determined by (27) (with (36) and (37–38)), the reduced excitation probabilities or corresponding strength functions

$$\begin{aligned} S_k(X\lambda\mu; \Delta T; E) &\equiv \sum_{\nu'} (\hbar\omega_\nu)^k |\langle \nu' | \hat{\mathcal{M}}_{X\lambda\mu}(\Delta T) | 0 \rangle|^2 \delta(E - \hbar\omega_\nu) \end{aligned} \quad (49)$$

can be determined. In order to simulate escape width and the coupling to complex configurations, the Dirac delta function in (49) is substituted by the Lorentz weight function $\delta_\Delta(E - \hbar\omega_\nu)$,

$$\delta_\Delta(E - \hbar\omega_\nu) = \frac{1}{2\pi} \frac{\Delta(E)}{(E - \hbar\omega_\nu)^2 + [\Delta(E)/2]^2}, \quad (50)$$

which averages locally the strength function in the energy dependent interval $\Delta(E)$. So the energy weighted strength function is taken in the form

$$\begin{aligned} S_k(X\lambda\mu; \Delta T; E) &\equiv \sum_{\nu'} (\hbar\omega_\nu)^k |\langle \nu' | \hat{\mathcal{M}}_{X\lambda\mu}(\Delta T) | 0 \rangle|^2 \delta_\Delta(E - \hbar\omega_\nu) \end{aligned} \quad (51)$$

with energy-dependent folding (see [32])

$$\Delta(E) = \begin{cases} \Delta_0 & \text{for } E \leq E_0 \\ \Delta_0 + a(E - E_0) & \text{for } E > E_0 \end{cases} \quad (52)$$

The form of the energy dependence in (52) is employed due to growth of the escape width and the coupling to complex configurations with increasing excitation energy E . Values of parameters Δ_0 and E_0 were fixed by the requirement of an agreement in the description of the experimental value of the photoabsorption cross section, which is discussed in the next section, where the spuriousity elimination effects in the strength functions of $E00$, $E1\mu$, $E1\mu com$, $E1\mu tor$, $E2\mu$ and $M1\mu$ excitations are discussed in detail as well.

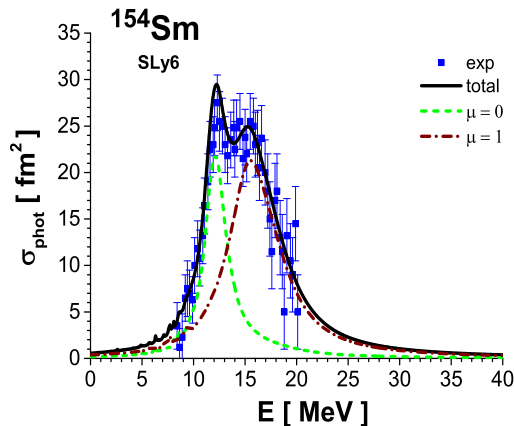


FIG. 1: Photoabsorption cross section in the dependence on the excitation energy, calculated in the framework of the BCS+QRPA approach with the Skyrme effective interaction SLy6, is compared with the corresponding experimental values taken from [35]. The cross section is determined by (53) where lorentzian averaging function (50), (52) was used in (51) with the parameters $\Delta_0 = 0.1$ MeV, $a = 0.15$, $E_0 = 8.3$ MeV.

III. DISCUSSION OF RESULTS

All calculations performed in this paper are made in the framework of the QRPA approach with the Skyrme effective interaction using the SLy6 parametrization [33]. The HF+BCS mean field was obtained by a stationary 2D calculation in the cylindrical coordinate, using a mesh size of 0.4 fm, and a box size of about three nuclear radii. The single-particle space is chosen to embrace the levels from the bottom of the potential well up to 40 MeV. For the Skyrme SLy6 parametrization in ^{154}Sm the single-particle scheme involves 1533 proton and 1729 neutron levels. The volume pairing interaction was used in the HF+BCS calculations and obtained equilibrium quadrupole deformation was $\beta = 0.339$. The subsequent QRPA calculations (see [34]), performed with the residual interactions containing the second functional derivatives of the total BCS energy with respect to all Skyrme and pairing densities, involve ≈ 7000 proton quasiparticle pairs and ≈ 12000 neutron quasiparticle pairs (in the case of the RPA calculation for $\mu^\pi = (\pm 1)^-$ which exhausts, together with $\mu^\pi = 0^-$, $\approx 95\%$ of the Thomas-Reiche-Kuhn EWSR for the E1 excitation).

Parameters $\Delta_0 = 0.1$ MeV, $a = 0.15$, and $E_0 = 8.3$ MeV of the lorentzian averaging function (50) were determined by the requirement of the agreement of the shape of the calculated photoabsorption cross section,

$$\sigma_{\text{phot}}(E) = \frac{16\pi^3 \alpha_{FS}}{9 e^2} \sum_{\mu=0, \pm 1} S_1(E1\mu; \Delta T = \text{nat}; E), \quad (53)$$

where $\alpha_{FS} = 1/137$ is the fine structure constant, with the corresponding experimental values. The compari-

son of calculated and experimental photoabsorption cross section is shown in the Fig.1. The good determination of these parameters is also checked in the Fig.2, where the experimental values of the isoscalar compression E1 energy weighted strength function $S_1(E1\mu \text{ com})$ is compared with the RPA-calculated Lorentz-averaged strength function, using the same parameters Δ_0 , a , and E_0 , and including the correction to the spurious elimination (see the subsection III A for more detailed discussion). One can see that the agreement for isoscalar ($\Delta T = 0$) compression E1 strength function is not perfect, but the overall features of E1 compression strength function are described with these parameters.

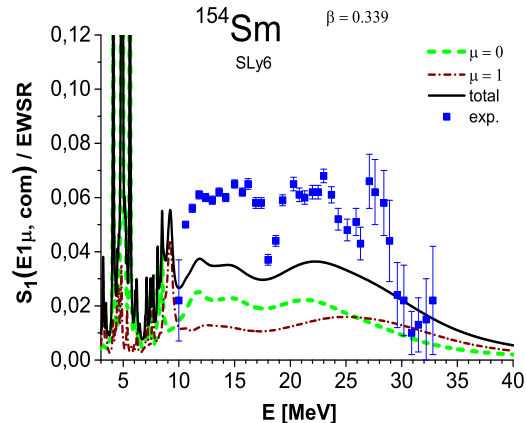


FIG. 2: Energy weighted strength function (49) of the isoscalar compression E1 transition operator (42) calculated by the Skyrme+QRPA approach with the SLy6 parametrization is compared with the corresponding experimental values taken from [36].

In the next subsection the spurious elimination is discussed for different types of excitations.

A. Elimination of the spuriousity from E1-type excitations

E1-type transitions include standard E1 excitations generated by the transition operator (41), compression E1 excitations generated by (42), and toroidal E1 excitations with the transition operator (43). Depending on the character of the process of excitation, the transition operator involves corresponding change of the isospin (ΔT), e.g. the photoabsorption corresponds to $\Delta T = \text{nat}$, or (α, α') reaction is related to $\Delta T = 0$ etc.

In the case of RPA states with $\mu^\pi = 0^-, 1^-$, the spuriousity is connected with the CoM translation motion. From the hermitian CoM cartesian coordinate vector, components of the rank-1 tensor can be constructed (gen-

eralized CoM coordinates $\hat{\mathcal{X}}_{0[\mu]}$ ($\mu = 0, \pm 1$),

$$\hat{\mathcal{X}}_{0[\mu]} = \sqrt{\frac{4\pi}{3}} \frac{1}{A} \sum_{j=1}^A r_j Y_{1\mu}(\hat{r}_j) \quad \mu = 0, \pm 1 \quad (54)$$

and the conjugated generalized linear momentum is

$$\hat{\mathcal{P}}_{0[\mu]} = -i\hbar \sum_{j=1}^A (\nabla_{\mu})_j \quad (55)$$

where $\nabla_0 = \frac{\partial}{\partial z}$, $\nabla_{\pm 1} = \mp \frac{1}{\sqrt{2}} (\frac{\partial}{\partial x} \pm i \frac{\partial}{\partial y})$ with $\nabla_{\mu}^{\dagger} = -(-1)^{\mu} \nabla_{-\mu}$. The operators (54) and (55) are conjugated, $[\hat{\mathcal{X}}_{0[\mu]}, \hat{\mathcal{P}}_{0[\mu]}^{\dagger}] = i\hbar$ (13), so the mode $(\hat{\mathcal{X}}_{0[\mu]}, \hat{\mathcal{P}}_{0[\mu]}^{\dagger})$, constructed from the CoM coordinate and linear momentum components, represents the spurious mode for the RPA equations with $\mu^{\pi} = 0^{-}$, $(\pm 1)^{-}$, and the corresponding spurious phonon is given by (19).

RPA Hamiltonian \hat{H}_{intr} has the form (18) which provides

$$[\hat{H}_{intr}, \hat{\mathcal{X}}_{0[\mu]}] = -\frac{i\hbar}{M_{0[\mu]}} \hat{\mathcal{P}}_{0[\mu]} \quad (56)$$

From the other side, one should realize that only kinetic-energy part of the Hamiltonian can contribute to the commutator $[\hat{H}_{intr}, \hat{\mathcal{X}}_{0[\mu]}]$, which on the other hand gives

$$\begin{aligned} & [\hat{H}_{intr}, \hat{\mathcal{X}}_{0[\mu]}] = \\ & = \left[\sum_{j=1}^A \sum_{\mu'} \frac{\hbar^2 (\nabla_{\mu'} \nabla_{\mu'}^{\dagger})_j}{2m}, \sqrt{\frac{4\pi}{3}} \frac{1}{A} \sum_{k=1}^A r_k Y_{1\mu}(\hat{r}_k) \right] = \\ & = -i \frac{\hbar}{mA} \hat{\mathcal{P}}_{0[\mu]} \end{aligned} \quad (57)$$

and the comparison of (56) with (57) gives the effective mass of the nucleus as $M_{0[\mu]} = mA$, where m is the nucleon mass.

Further, we show that in the case of the isoscalar E1 transitions, generated by the operator $\hat{\mathcal{M}}_{E1\mu}^{(\Delta T=0)} = \sum_{j=1}^A e_{\Delta T=0}^{(j)} r_j Y_{1\mu}(\hat{r}_j) = \frac{1}{2} \sum_{j=1}^A r_j Y_{1\mu}(\hat{r}_j)$, the whole energy-weighted sum rule (EWSR) strength, defined as

$$\begin{aligned} m_1(\mathcal{M}_{X\lambda\mu}, \Delta T) &= \int_0^{\infty} dE S_1(X\lambda\mu; \Delta T; E) = \\ &= \sum_{\nu} \hbar\omega_{\nu[\mu]} |\langle \nu | \hat{\mathcal{M}}_{X\lambda\mu}^{(\Delta T)} | 0 \rangle|^2, \end{aligned} \quad (58)$$

is exhausted by the spurious mode only. The spurious mode part of the $m_1(\mathcal{M}_{X1\mu}, \Delta T=0)$ is (see (19), (54),

and $M_{0[\mu]} = mA$)

$$\begin{aligned} m_1(\mathcal{M}_{X1\mu}, \Delta T=0) &= \\ &= \hbar\omega_{s[\mu]} |\langle RPA | [Q_{s[\mu]}, \frac{1}{2} \sum_{j=1}^A r_j Y_{1\mu}(\hat{r}_k)] | 0 \rangle|^2 = \\ &= \hbar\omega_{s[\mu]} \frac{3(A/2)^2}{16\pi\hbar^2 x_s^2[\mu]} |\langle 0 | [\hat{\mathcal{P}}_{0[\mu]}^{\dagger}, \hat{\mathcal{X}}_{0[\mu]}] | 0 \rangle|^2 = \\ &= \frac{3\hbar^2}{8\pi m} \frac{A}{4} \end{aligned} \quad (59)$$

Therefore, the spurious mode exhaust the whole TRK EWSR value $\frac{3\hbar^2}{8\pi m} \frac{A}{4}$ for isoscalar $E1\mu$ excitation, corresponding to operator $\frac{1}{2} \sum_{j=1}^A r_j Y_{1\mu}(\hat{r}_j)$. It also means that there aren't any physical $E1\mu$ isoscalar states excited by that operator, because all isoscalar $E1\mu$ strength is exhausted by the spurious mode connected with the CoM translation motion. This conclusion will be moreover supported by the fact that the corrected matrix element (32) of a time-odd operator $t_q(\vec{r}) = r^0 \vec{Y}_{1\mu}^0 = \vec{e}_{\mu}/\sqrt{4\pi}$ (constant vector) has zero value for all physical non-spurious states ν' (i.e., the isoscalar $E1\mu$ transition current averages to zero).

In the following, we determine the transition matrix element of the long-wave $E1$ transition operator for so-called natural case, generated by the transition operator $\hat{\mathcal{M}}_{E1\mu}^{(\Delta T=nat)} = \sum_{j=1}^A e_{\Delta T=nat}^{(j)} r_j Y_{1\mu}(\hat{r}_j) = \sum_{j=1}^Z r_j Y_{1\mu}(\hat{r}_j)$ where only protons contribute. Equation (28) gives

$$\begin{aligned} \langle \nu' | \hat{T}_q | 0 \rangle &= \int d^3r \delta\rho_{\nu';q}(\vec{r}) r Y_{1\mu}(\hat{r}) = \\ &= \int d^3r \delta\rho_{\nu;q}(\vec{r}) r Y_{1\mu}(\hat{r}) - y_{\nu} \int d^3r \delta\rho_{s;q}(\vec{r}) r Y_{1\mu}(\hat{r}) \end{aligned} \quad (60)$$

with y_{ν} defined by (29). Here, the spurious coordinate operator is proportional to the isoscalar E1 transition operator (see (54)), so the factor y_{ν} can be rewritten as follows

$$y_{\nu}^{(\mu)} = \frac{\int d^3r \delta\rho_{\nu[\mu];0}(\vec{r}) r Y_{1\mu}(\hat{r})}{\int d^3r \delta\rho_{s[\mu];0}(\vec{r}) r Y_{1\mu}(\hat{r})} \quad (61)$$

with

$$\begin{aligned} \delta\rho_{s[\mu];q}(\vec{r}) &= \langle 0 | [Q_{s[\mu]}, \hat{\rho}_q(\vec{r})] | 0 \rangle = \\ &= \frac{i}{2\hbar x_s} \langle 0 | [\hat{\mathcal{P}}_{0[\mu]}^{\dagger}, \hat{\rho}_q(\vec{r})] | 0 \rangle = \\ &= \frac{1}{2x_s} (-1)^{\mu} \nabla_{-\mu} \rho_{BCS;q}(\vec{r}) \end{aligned} \quad (62)$$

where $\rho_{BCS;q}(\vec{r})$ is the BCS ground state single-quasiparticle density, and will be normalized according to the type of the transition ($\Delta T = nat, 0, 1$) as $\int d^3r \rho_{BCS;\Delta T=nat}(\vec{r}) = Z$, $\int d^3r \rho_{BCS;\Delta T=0}(\vec{r}) = A/2$ and $\int d^3r \rho_{BCS;\Delta T=1}(\vec{r}) = (Z - N)/2$. Then, using (62),

the identity $(-1)^\mu \nabla_{-\mu} r Y_{1\mu}(\vec{r}) = \sqrt{\frac{3}{4\pi}}$ for all μ , and *per partes* integration, the denominator in (61) obtains the following form,

$$\int d^3r \delta\rho_{s; \Delta T=0}(\vec{r}) r Y_{1\mu}(\hat{r}) = \frac{-1}{2x_s} \sqrt{\frac{3}{4\pi}} \frac{A}{2} \quad (63)$$

and the last integral in (60) is

$$\int d^3r \delta\rho_{s; \Delta T=nat}(\vec{r}) r Y_{1\mu}(\hat{r}) = \frac{-1}{2x_s} \sqrt{\frac{3}{4\pi}} Z \quad (64)$$

Finally, the substitution of (64), (63) into (60) gives the transition matrix element in the following form

$$\begin{aligned} \langle \nu' | \hat{\mathcal{M}}_{E1\mu}^{(\Delta T=nat)} | 0 \rangle &= \\ &= \int d^3r \delta\rho_{\nu; \Delta T=nat}(\vec{r}) r Y_{1\mu}(\hat{r}) \\ &\quad - \frac{2Z}{A} \int d^3r \delta\rho_{\nu; \Delta T=0}(\vec{r}) r Y_{1\mu}(\hat{r}) = \\ &= \frac{N}{A} \int d^3r \delta\rho_{\nu; p}(\vec{r}) r Y_{1\mu}(\hat{r}) \\ &\quad - \frac{Z}{A} \int d^3r \delta\rho_{\nu; n}(\vec{r}) r Y_{1\mu}(\hat{r}) \end{aligned} \quad (65)$$

where $\delta\rho_{\nu, q}(\vec{r})$ for $q = prot, neut$ is given by (30) for $\mu^\pi = 0^-$ and 1^- .

Expression (65) is the standard expression for the matrix element of the electric transition operator $\hat{\mathcal{M}}_{E1\mu}^{(\Delta T=nat)}$ (with only proton contribution) where CoM spurious mode is eliminated by the special choice of effective charges $e_p = \frac{N}{A}$ and $e_n = -\frac{Z}{A}$ (see e.g. [8]). So, our scheme of elimination of spuriousity is in agreement with these well-known effective charges.

All calculations presented in this paper are focused mainly on axially deformed nuclei. Therefore, the best way to calculate integrals in (61) is to use a cylindrical coordinate frame. In such a case we should express $r Y_{1\mu}(\hat{r})$ in the cylindrical coordinates. It will be done for general dipole operator $f(r) Y_{1\mu}(\vec{r})$, where $f(r)$ is arbitrary radial function of the vector modulus $r = \sqrt{\varrho^2 + z^2}$ (here $\vec{r} \equiv \varrho, z, \phi$ are cylindrical coordinates). In general, we can write (see Appendix A for details)

$$f(r) Y_{\lambda\mu}(\hat{r}) = f_{\lambda\mu}(\varrho, z) e^{i\mu\phi} \quad (66)$$

where functions $f_{\lambda\mu}(\varrho, z) = (-1)^\mu f_{\lambda, -\mu}(\varrho, z)$ for $\lambda = 1$ and 2 and for given radial function $f(r = \sqrt{\varrho^2 + z^2})$ are given in Appendix A (see (A.2) and (A.4)). Similarly, the transition density $\delta\rho_{\nu[\mu]; q}(\vec{r})$ can be expressed in the cylindrical coordinates as $\delta\rho_{\nu[\mu]; q}(\vec{r}) = \delta\rho_{\nu; q}^{(\mu)}(\varrho, z) e^{-i\mu\phi}$. Then the integrals in (65) are

$$\begin{aligned} \int d^3r \delta\rho_{\nu[\mu]; q}(\vec{r}) r Y_{1\mu}(\vec{r}) &= \\ &= 2\pi \int dz \int d\varrho \varrho \delta\rho_{\nu; q}^{(\mu)}(\varrho, z) f_{1\mu}^{(1)}(\varrho, z) \end{aligned} \quad (67)$$

where $f_{1\mu}^{(1)}(\varrho, z)$ is given by (A.2) for the function $f(r) = r = \sqrt{\varrho^2 + z^2}$.

Next, we analyze the elimination of spuriousity from the compression $E1$ excitations. These excitations are defined by the transition operator (42) which is related to the second-order term in the long-wave decomposition of the total electric $E1$ transition operator (where the leading first-order term is the long-wave $E1$ transition operator (41) – see [9] for details). Corrected matrix element (28) of operator (42) gives

$$\begin{aligned} \langle \nu' | \hat{\mathcal{M}}_{E1\mu com}^{(\Delta T)} | 0 \rangle &= \\ &= \frac{1}{10} \int d^3r (\delta\rho_{\nu[\mu]; \Delta T}(\vec{r}) - y_{\nu[\mu]} \delta\rho_{s[\mu]; \Delta T}(\vec{r})) r^3 Y_{1\mu}(\hat{r}) \end{aligned} \quad (68)$$

where $y_{\nu[\mu]}$ is again given by (61). The substitution of (62) in (61) and subsequently in (68), and using *per partes* integration yields,

$$\begin{aligned} \langle \nu' | \hat{\mathcal{M}}_{E1\mu com}^{(\Delta T)} | 0 \rangle &= \\ &= \frac{1}{10} \int d^3r \left\{ \delta\rho_{\nu[\mu]; \Delta T}(\vec{r}) \right. \\ &\quad \left. - \sqrt{\frac{4\pi}{3}} \frac{2}{A} \left[\int d^3r' \delta\rho_{\nu[\mu]; 0}(\vec{r}') r' Y_{1\mu}(\hat{r}') \right] \right. \\ &\quad \left. \rho_{BCS; \Delta T}(\vec{r}) (-1)^\mu \nabla_{-\mu} \right\} r^3 Y_{1\mu}(\hat{r}) \end{aligned} \quad (69)$$

We will determine $\nabla_{-\mu} r^3 Y_{1\mu}(\hat{r})$. According to expressions (5.8.10–11) in [30], the following identities hold

$$\begin{aligned} \nabla_0 r^3 Y_{10}(\hat{r}) &= \frac{1}{\sqrt{3}} \left[5r^2 Y_{00} + \frac{4}{\sqrt{5}} r^2 Y_{20}(\hat{r}) \right] \\ \nabla_1 r^3 Y_{1,-1}(\hat{r}) &= \nabla_{-1} r^3 Y_{11}(\hat{r}) = \\ &= \frac{1}{\sqrt{3}} \left[-5r^2 Y_{00} + \frac{2}{\sqrt{5}} r^2 Y_{20}(\hat{r}) \right] \end{aligned} \quad (70)$$

and the substitution of (70) into (69) gives

$$\begin{aligned} \langle \nu' | \hat{\mathcal{M}}_{E1\mu com}^{(\Delta T)} | 0 \rangle &= \\ &= \frac{1}{10} \sum_{q=p,n} \left\{ \int d^3r e_q \delta\rho_{\nu[\mu]; q}(\vec{r}) r^3 Y_{1\mu}(\hat{r}) \right. \\ &\quad \left. - \frac{\sqrt{4\pi}}{3} \frac{2}{A} \left[\int d^3r' \delta\rho_{\nu[\mu]; 0}(\vec{r}') r' Y_{1\mu}(\hat{r}') \right] \right. \\ &\quad \times e_q \int d^3r \rho_{BCS; q}(\vec{r}) r^2 \\ &\quad \left. \times \left[5 Y_{00} + \left\{ \begin{array}{l} 4 \text{ (for } \mu = 0) \\ -2 \text{ (for } \mu = \pm 1) \end{array} \right\} \frac{1}{\sqrt{5}} Y_{20}(\hat{r}) \right] \right\} \end{aligned} \quad (71)$$

and finally the transformation to cylindrical coordinates

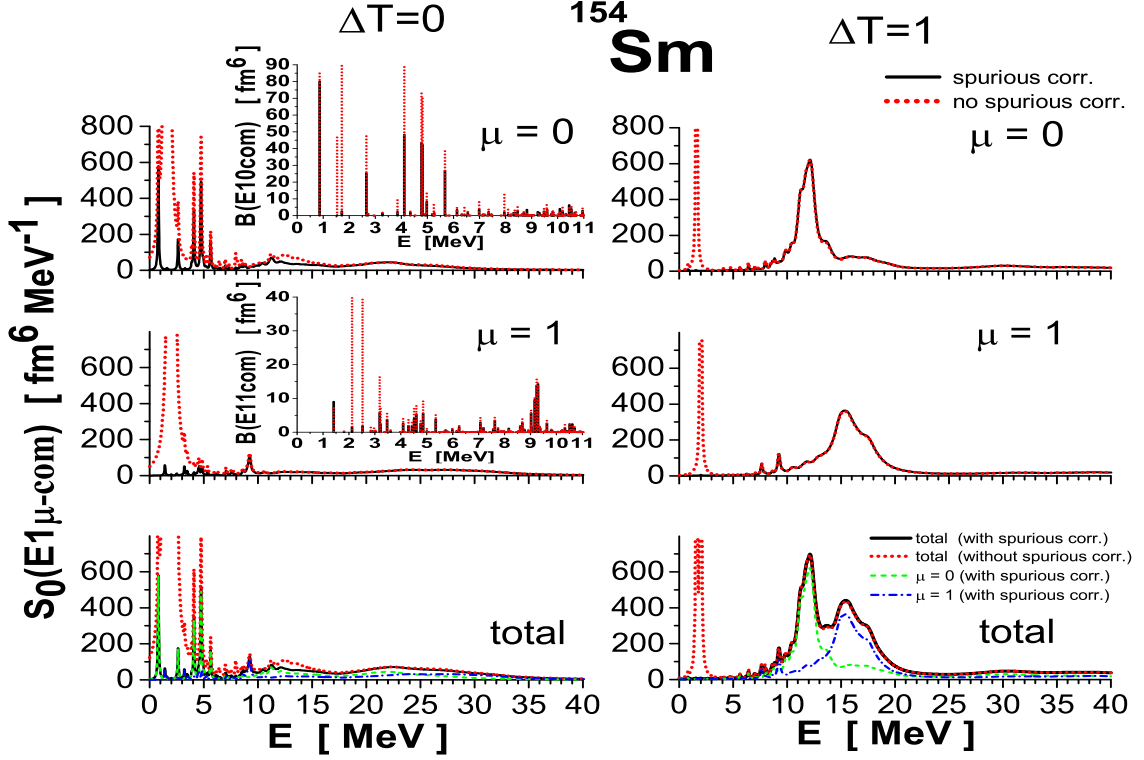


FIG. 3: Strength function (49) of the isoscalar (left panels) and isovector (right panels) compression E1 transition operator (42) calculated with the Skyrme+RPA approach using the SLy6 parametrization. Upper panels involve angular momentum component $\mu = 0$, middle panels correspond to $\mu = \pm 1$ and lower panels contain the total strength function summed over all μ . Red dotted curves were obtained by the calculations without spuriocity elimination and black solid lines were obtained with the spuriocity-elimination corrections. Insets in the left upper panels for $\mu = 0$ and $\mu = 1$ show the reduced excitation probabilities $B(E10\ com)$ and $B(E11\ com)$ from the RPA vacuum to the lowest RPA solutions (with the excitation energies up to 11 MeV). In the lower panels green dotted curves and blue dot-dashed curves correspond to $\mu = 0$ and $\mu = \pm 1$ parts of the strength function, respectively.

yields

$$\begin{aligned}
 \langle \nu' | \hat{\mathcal{M}}_{E1\mu\ com}^{(\Delta T)} | 0 \rangle &= \\
 &= \frac{1}{10} \sum_{q=p,n} \left\{ \int dz \int d\rho 2\pi\rho \delta\rho_{\nu;q}^{(\mu)}(\rho, z) \left[e_q f_{1\mu}^{(3)}(\rho, z) \right. \right. \\
 &\quad - \frac{5}{3} \langle r^2 \rangle_{\Delta T} f_{1\mu}^{(1)}(\rho, z) \\
 &\quad \left. \left. - \left\{ \begin{array}{l} 4 \text{ (for } \mu = 0) \\ -2 \text{ (for } \mu = \pm 1) \end{array} \right\} \frac{\sqrt{4\pi}}{3\sqrt{5}} \langle r^2 Y_{20} \rangle_{\Delta T} f_{1\mu}^{(1)}(\rho, z) \right] \right\} \\
 &\quad (72)
 \end{aligned}$$

where

$$\begin{aligned}
 \langle r^2 \rangle_{\Delta T} &\equiv \frac{1}{A} \sum_{q=p,n} e_q \int d^3r \rho_{BCS;q}(\vec{r}) r^2 \\
 \langle r^2 Y_{20} \rangle_{\Delta T} &\equiv \frac{1}{A} \sum_{q=p,n} e_q \int d^3r \rho_{BCS;q}(\vec{r}) r^2 Y_{20}(\hat{r}) \\
 &= \sqrt{\frac{5}{16\pi}} \langle r^2 (3 \cos^2 \theta - 1) \rangle_{\Delta T} \approx \frac{5}{4\pi} \beta \langle r^2 \rangle_{\Delta T} \\
 &\quad (73)
 \end{aligned}$$

where $f_{1\mu}^{(1)}(\rho, z)$ are given by (A.2) for $f(r) = r = \sqrt{\rho^2 + z^2}$ and functions $f_{1\mu}^{(3)}(\rho, z)$ are given by (A.2) for $f(r) = r^3 = (\rho^2 + z^2)^{3/2}$.

One should realize that the second term in (72) corresponds precisely to the correction term for the elimination of the spuriocity in the compression E1 transitions derived for the spherical nuclei (see e.g. [8]). The last term is connected with the nonzero deformation. The fact that for the spherical nuclei our spuriocity elimination method gives the well-known correction term for the compression E1 transition operator is again a confirmation of our approach.

In the Fig.3 we demonstrate the elimination of the CoM spuriocity for the nucleus ^{154}Sm in the isoscalar (left panels) and isovector (right panels) compression E1 μ excitation strength functions $S_0(E1\mu\ com; \Delta T = 0, 1; E)$ (49), while we show $\mu = 0$ in top panels, $\mu = \pm 1$ in middle panels and total, i.e., sum over all μ in lower panel. The black solid curves in all panels correspond to the Skyrme BCS+QRPA calculations involving the spuriocity elimination corrections (32), and the red dotted curves represent results without any spuriocity cor-

rections. In the bottom panels, with the $E1$ compression strength function – as total and separate $\mu = 0, \pm 1$, including the CoM spuriousity corrections (green dashed curves for $\mu = 0$ and blue dash-dotted curves for $\mu = \pm 1$). The huge CoM spuriousity elimination effect can be seen in all panels of the Fig.3 for the lowest spurious peak. Besides the spurious peak, the spuriousity admixtures from other low-lying phonon states are eliminated (especially for isoscalar $\Delta T = 0$ excitations). Calculations confirm also expected fact that excitations with higher energy do not contain spuriousity admixtures. The only exception is the energy region 11–15 MeV for $\Delta T = 0$ $E10\text{ com}$ excitations with $\mu = 0$ where the differences between red dotted and black solid lines are observed.

The toroidal $E1$ transition operator $\hat{\mathcal{M}}_{E1\mu\text{ tor}}(\Delta T)$ (43) generating toroidal character of $E1$ excitations is directly related to the $E1$ compression operator (see [9]) and therefore is also the second order operator in the long-wave decomposition of the total electric $E1$ operator. Since the nucleon current $\hat{j}_{nuc;\Delta T}(\vec{r})$ involved in $\hat{\mathcal{M}}_{E1\mu\text{ tor}}(\Delta T)$ is the time-odd operator with $\gamma_T^{(\hat{j}_{nuc})} = -1$ ($\mathcal{T}^{-1} \hat{j}_{nuc;\Delta T}(\vec{r}) \mathcal{T} = -\hat{j}_{nuc;\Delta T}(\vec{r})$), $\hat{j}_{nuc;\Delta T}^{\dagger}(\vec{r}) = \hat{j}_{nuc;\Delta T}(\vec{r})$ and because of the well known relations for the vector spherical harmonics $\vec{Y}_{1\mu}^0(\vec{r})$ and $\vec{Y}_{1\mu}^2(\vec{r})$ ($\vec{Y}_{1\mu}^{0*}(\hat{r}) = (-1)^\mu \vec{Y}_{1,-\mu}^0(\hat{r})$, $\vec{Y}_{1\mu}^{2*}(\hat{r}) = (-1)^\mu \vec{Y}_{1,-\mu}^2(\hat{r})$) the transition toroidal $E1$ operator (43) is time-odd in the sense of (8) with $\gamma_T^{(\mathcal{M}_{E1\mu\text{ tor}})} = -1$. Therefore the spurious-elimination-corrected matrix element (32) of this operator reads

$$\begin{aligned} \langle \nu' | \hat{\mathcal{M}}_{E1\mu\text{ tor}}^{(\Delta T)} | 0 \rangle &= \\ &= -\frac{i}{2\sqrt{3}} \int d^3r \left(\delta \vec{j}_{\nu[\mu];\Delta T}(\vec{r}) - z_{\nu[\mu]} \delta \vec{j}_{s[\mu];\Delta T}(\vec{r}) \right) \times \\ &\quad \times r^2 \left(\vec{Y}_{1\mu}^0(\hat{r}) + \frac{\sqrt{2}}{5} \vec{Y}_{1\mu}^2(\hat{r}) \right) \end{aligned} \quad (74)$$

where transition currents $\delta \vec{j}_{\nu[\mu];\Delta T}(\vec{r})$ and $\delta \vec{j}_{s[\mu];\Delta T}(\vec{r})$ are given by

$$\delta \vec{j}_{\nu[\mu];\Delta T}(\vec{r}) \equiv \langle 0 | [Q_{\nu[\mu]}, \hat{j}_{nuc;\Delta T}(\vec{r})] | 0 \rangle \quad (75a)$$

$$\delta \vec{j}_{s[\mu];\Delta T}(\vec{r}) \equiv \langle 0 | [\hat{\mathcal{X}}_{0[\mu]}^+, \hat{j}_{nuc;\Delta T}(\vec{r})] | 0 \rangle \quad (75b)$$

with $\hat{\mathcal{X}}_{0[\mu]}$ introduced by (54). Further, we will treat only the convective part of the nucleon current (see (46)), because magnetization part commutes with \hat{X}_0 , which doesn't contain spin.

$$\hat{j}_{conv;\Delta T}(\vec{r}) = -\frac{i\hbar}{mc} \sum_{j=1}^A \frac{e_{\Delta T}^{(j)}}{2} [\delta(\vec{r} - \vec{r}_j) \vec{\nabla}_j + \vec{\nabla}_j \delta(\vec{r} - \vec{r}_j)] \quad (76)$$

Then the expression (75b) can be rewritten as follows (using (54) and identities from the subsection 7.3.4 in [30]),

$$\begin{aligned} \delta \vec{j}_{s[\mu];\Delta T}(\vec{r}) &= -\frac{i\hbar}{mcA} \sqrt{\frac{4\pi}{3}} \langle 0 | \left[\sum_i r_i Y_{1\mu}^*(\hat{r}_i), \right. \\ &\quad \left. \frac{1}{2} \sum_j e_{\Delta T}^{(j)} [\delta(\vec{r} - \vec{r}_j) \vec{\nabla}_j + \vec{\nabla}_j \delta(\vec{r} - \vec{r}_j)] \right] | 0 \rangle = \\ &= \frac{i\hbar}{mcA} \sqrt{4\pi} \vec{Y}_{1\mu}^{0*}(\hat{r}) \sum_{j=1}^A e_{\Delta T}^{(j)} \langle 0 | \delta(\vec{r} - \vec{r}_j) | 0 \rangle = \\ &= \frac{i\hbar}{mcA} \sqrt{4\pi} \rho_{BCS;\Delta T}(\vec{r}) \vec{Y}_{1\mu}^{0*}(\hat{r}) \end{aligned} \quad (77)$$

The factor $z_{\nu[\mu]}$ in (74) is calculated by the prescription (33), while realizing that

$$\hat{P}_{0[\mu]} = mc \int d^3r 2 \hat{j}_{conv;\Delta T=0} \cdot \vec{e}_\mu \quad (78)$$

Such procedure is equivalent to the requirement that the current of all free-of-spuriousity intrinsic $E1$ isoscalar ($\Delta T = 0$) excitations $|\nu'\rangle$ should be zero (and in accordance with (59) all isoscalar $E1\mu$ EWSR is exhausted only by the CoM spurious state). One should realize that the spuriousity for $E1\mu$ transitions is connected with the translation of the whole nucleus and it is clear that the projection of the corrected density of corresponding convective current onto the vector $\vec{Y}_{1\mu}^0 = \frac{\vec{e}_\mu}{\sqrt{4\pi}}$, (where $\vec{e}_{\mu=0} = \vec{e}_z$, $\vec{e}_{\mu=\pm 1} = \frac{\mp 1}{\sqrt{2}}(\vec{e}_x \pm i\vec{e}_y)$) integrated over all nucleus volume should be zero. So the condition of the elimination of the spuriousity current can be rewritten as (using (77) and the identity $\vec{Y}_{1\mu}^{0*} \cdot \vec{Y}_{1\mu}^0 = \frac{1}{4\pi}$),

$$\begin{aligned} 0 &= \int d^3r (\delta \vec{j}_{\nu;\Delta T=0}(\vec{r}) - z_{\nu[\mu]} \delta \vec{j}_{s;\Delta T=0}(\vec{r})) \cdot \vec{Y}_{1\mu}^0(\hat{r}) \\ &= \frac{1}{\sqrt{4\pi}} \left(2 \int d^3r \delta \vec{j}_{\nu;\Delta T=0}(\vec{r}) \cdot \vec{e}_\mu - z_{\nu[\mu]} \frac{i\hbar}{mc} \right) \\ &\Rightarrow z_{\nu[\mu]} = -\frac{imc}{\hbar} \int d^3r 2 \delta \vec{j}_{\nu;\Delta T=0}(\vec{r}) \cdot \vec{e}_\mu \end{aligned} \quad (79)$$

The substitution of (79) and (77) into (74) gives the following expression for the corrected excitation matrix elements of toroidal $E1$ operator,

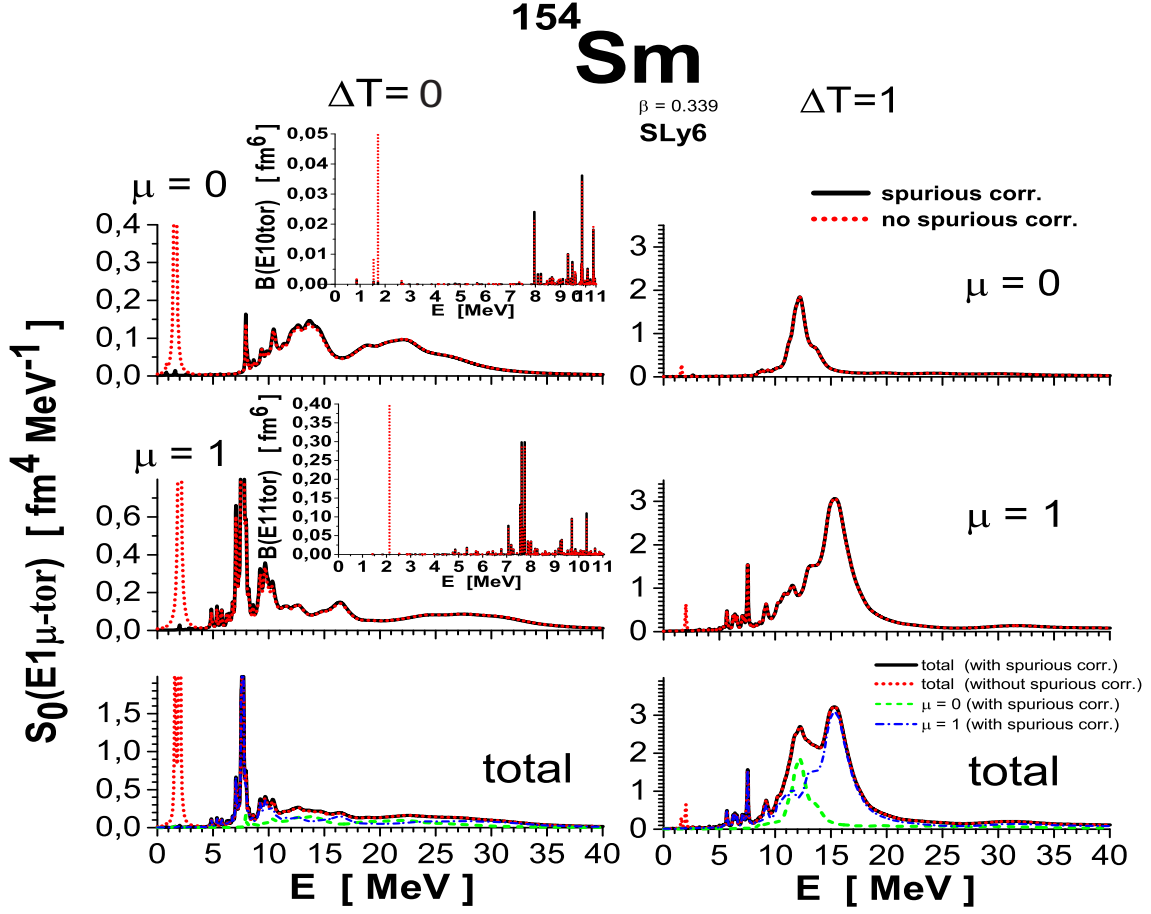


FIG. 4: The same as in the Fig.3 but for the strength function of toroidal $E1$ excitations.

$$\begin{aligned}
\langle \nu' | \hat{\mathcal{M}}_{E1\mu\text{tor}}^{(\Delta T)} | 0 \rangle = & -\frac{i}{2\sqrt{3}} \times \left\{ \int d^3r \left[\delta \vec{j}_{\nu[\mu]; \Delta T}(\vec{r}) \cdot r^2 \vec{Y}_{1\mu}^0(\hat{r}) - \left(\frac{2}{A} \int d^3r' \rho_{BCS; \Delta T}(\vec{r}') r'^2 \right) \delta \vec{j}_{\nu; \Delta T=0}(\vec{r}) \cdot \vec{Y}_{1\mu}^0 \right] \right. \\
& \left. + \frac{\sqrt{2}}{5} \int d^3r \left[\delta \vec{j}_{\nu[\mu]; \Delta T}(\vec{r}) \cdot r^2 \vec{Y}_{1\mu}^2(\hat{r}) - 4\pi \left(\frac{2}{A} \int d^3r' \rho_{BCS; \Delta T}(\vec{r}') r'^2 \vec{Y}_{1\mu}^{0*} \cdot \vec{Y}_{1\mu}^2(\vec{r}') \right) \delta \vec{j}_{\nu; \Delta T=0}(\vec{r}) \cdot \vec{Y}_{1\mu}^0 \right] \right\} \quad (80)
\end{aligned}$$

Further we can rewrite (80) using the relation

$$\vec{Y}_{1\mu}^{0*} \cdot \vec{Y}_{1\mu}^2(\hat{r}) = \frac{3(-1)^{\mu+1}}{\sqrt{4\pi}} \begin{Bmatrix} 1 & 1 & 2 \\ 2 & 0 & 1 \end{Bmatrix} C_{00\ 20}^{20} C_{1-\mu\ 1\mu}^{20} Y_{20}(\hat{r}) = \frac{Y_{20}(\hat{r})}{\sqrt{40\pi}} c_{\mu} = \frac{3 \cos^2 \theta - 1}{8\pi\sqrt{2}} c_{\mu} = \frac{2z^2 - \rho^2}{8\pi\sqrt{2}} \quad (81)$$

following from the identity (7.3.100) in [30]. In (81) $c_0 = -2$ and $c_{\pm 1} = 1$. The resultant expressions of corrected matrix elements $\langle \nu' | \hat{\mathcal{M}}_{E1\mu\text{tor}}^{(\Delta T)} | 0 \rangle$ are

$$\begin{aligned}
\langle \nu' | \hat{\mathcal{M}}_{E10\text{tor}}^{(\Delta T)} | 0 \rangle = & -\frac{i}{2c\sqrt{3}} \int d^3r \left\{ \delta \vec{j}_{\nu[0]; \Delta T}(\vec{r}) \cdot \left[r^2 \vec{Y}_{10}^0 + \frac{\sqrt{2}}{5} r^2 \vec{Y}_{10}^2(\hat{r}) \right] \right. \\
& \left. - \left[\langle r^2 \rangle_{\Delta T} - \frac{1}{5} \langle r^2 (3 \cos^2 \theta - 1) \rangle_{\Delta T} \right] \left[\delta \vec{j}_{\nu[0]; p}(\vec{r}) + \delta \vec{j}_{\nu[0]; n}(\vec{r}) \right] \cdot \vec{Y}_{10}^0 \right\} \quad (82a)
\end{aligned}$$

$$\begin{aligned}
\langle \nu' | \hat{\mathcal{M}}_{E11\text{ tor}}^{(\Delta T)} | 0 \rangle = & -\frac{i}{2c\sqrt{3}} \int d^3r \left\{ \delta \vec{J}_{\nu[1]; \Delta T}(\vec{r}) \cdot \left[r^2 \vec{Y}_{11}^0 + \frac{\sqrt{2}}{5} r^2 \vec{Y}_{11}^2(\hat{r}) \right] \right. \\
& \left. - \left[\langle r^2 \rangle_{\Delta T} - \frac{1}{10} \langle r^2 (3 \cos^2 \theta - 1) \rangle_{\Delta T} \right] [\delta \vec{J}_{\nu[1]; p}(\vec{r}) + \delta \vec{J}_{\nu[1]; n}(\vec{r})] \cdot \vec{Y}_{11}^0 \right\}
\end{aligned} \tag{82b}$$

so the c.m.c. amounts to a modification of radial $\vec{Y}_{1\mu}^0$ part of the transition operator, similarly to the spherical case.

The Fig.4 demonstrates the CoM elimination effect for the toroidal $E1$ excitations generated by the operator (43). The description of curves in all panels is the same as in the Fig.3. In the case of $E1$ toroidal excitations the whole spurious peaks for $\Delta T = 0$ and $\Delta T = 1$ $E1$ toroidal transitions are eliminated. In contrast to the compression $E1$ excitations in the Fig.3, the non-spurious toroidal RPA $E1$ excitations contain no spurious admixtures (black solid and red dotted curves coincide).

B. Elimination of the spuriosity from $E0$ and $E20$ excitations

In the case of the electric monopole $E0$ and electric quadrupole $E20$ excitations with the ang. momentum projection $\mu = 0$ the spuriosity is connected with the symmetry of the total intrinsic Hamiltonian with respect to the number of particle conservation, namely with the requirement

$$[\hat{H}_{intr}, \hat{N}] = 0 \tag{83}$$

Since the number of particle operator is time-even (symmetric with respect to the time-reverse operator \mathcal{T} , $\mathcal{T}^{-1} \hat{N} \mathcal{T} = \hat{N}$) we cannot identify the number of particle operator \hat{N} with the time-odd operator $\hat{\mathcal{P}}_0$ of generalized linear momentum with the zero (or close to zero) energy but with the corresponding conjugated generalized coordinate $\hat{\mathcal{X}}_0$ of the spurious mode, $\hat{\mathcal{X}}_0 \equiv \hat{N}$. In the framework of the two-quasiparticle approximation the number of particle operator $\hat{N} = \sum_i a_i^+ a_i$ is expressed in terms of quasiparticle operators α_i^+ , α_i as follows,

$$\hat{\mathcal{X}}_0 = \hat{N} = 2 \sum_{j>0} \mathcal{U}_j \mathcal{V}_j (\alpha_j^+ \alpha_j^+ + \alpha_j^- \alpha_j^-) \tag{84}$$

with two-quasiparticle amplitudes $\mathcal{X}_{ij}^{(0)} = \mathcal{X}_{ij}^{(0)*} = 2 \mathcal{U}_i \mathcal{V}_i \delta_{ij}$. In (84) \mathcal{U}_i and \mathcal{V}_i are BCS pairing occupation amplitudes. The two-quasiparticle amplitudes $\mathcal{P}_{ij}^{(0)} = \langle ij | \hat{\mathcal{P}}_0 | 0 \rangle$ of the conjugated linear momentum, $\hat{\mathcal{P}}_0 = \sum_{ij} \mathcal{P}_{ij}^{(0)} (\alpha_i^+ \alpha_j^+ - \alpha_j^- \alpha_i^-)$, are given by (35). Then the transition matrix elements $\langle \nu' | \hat{T}_q | 0 \rangle$ of any time-even transition operator (like the monopole $E0$ transition operator (39)) between the physical spurious free states $|\nu'\rangle$ and the RPA phonon vacuum $|0\rangle$ are determined by (28)

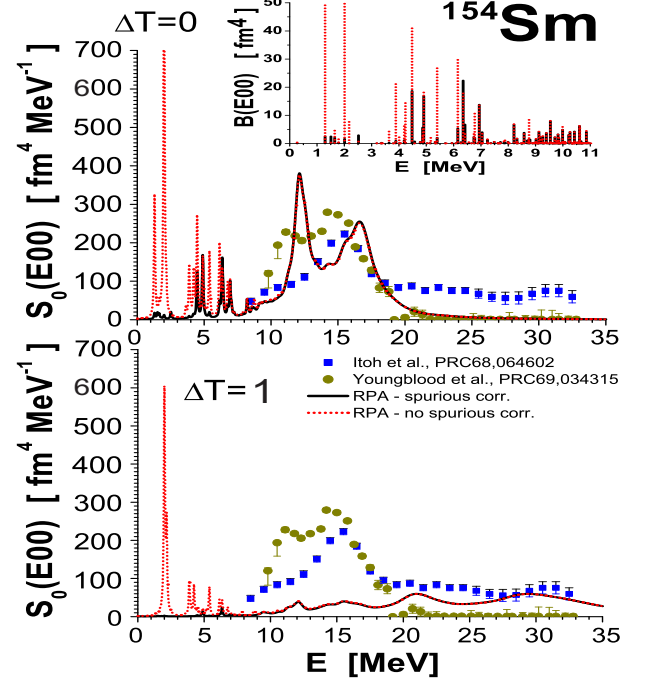


FIG. 5: Strength function (49) of the isoscalar (upper panel) and isovector (lower panel) electric monopole $E0$ transition operator calculated with the SLy6 Skyrme+RPA approach. Red dotted curves were obtained by the calculation without spuriosity elimination and black solid lines were obtained by including the spuriosity-elimination corrections. The experimental values, taken from [37]-blue squares and [36]- yellow circles, were claimed to be of isoscalar $E0$ character. The inset in the upper panel for the $\Delta T = 0$ transitions shows the reduced probabilities of excitations from the RPA ground state to the lowest excitations (with energies up to 11 MeV) calculated with the spuriosity-elimination corrections (black columns) and without corrections (dotted red columns).

where $Q_s^{\dagger} = x_s \hat{N} - \frac{i}{2\hbar x_s} \hat{\mathcal{P}}_0$. It should be mentioned here that the previous “heuristic” prescription of the number of particle spuriosity elimination introduced in [11] used directly $\hat{\mathcal{P}}_{ij}^{(0)} = N_{ij} = 2\mathcal{U}_i \mathcal{V}_i \delta_{ij}$, that means the role of $\hat{\mathcal{P}}_0$ and $\hat{\mathcal{X}}_0$ are not distinguished.

The Fig.5 shows the effect of the elimination of the spuriosity from the isoscalar and isovector $E0$ excitation strength function. Calculated isoscalar $E0$ strength function is compared with experimental one [36, 37] in the

upper panel. One can see that the relative agreement of calculated and experimental values in the GMR region but the high energy interval (for excitation energy $E > 20$ MeV) is described by the calculation only for experimental data of [36]. In the bottom panel the isovector E0 strength function is shown. In the papers [36, 37] authors claimed that (α, α') reaction used for the extraction of E0 strength gave predominantly isoscalar E0 strength. However, it is not fully excluded that (α, α') reaction partly excites also isovector modes and therefore the experimental data from [36, 37] are shown also in the bottom panel with isovector E0 strength function. In both top and bottom panels not only spurious peak with the lowest energy is eliminated by our approach but also the spurious admixtures in other low-lying RPA states are eliminated. However, in the regions of isoscalar and isovector GMR the solid black and dotted red curves coincide which is the indication that in high excitation energies the RPA states do not contain spurious admixtures.

The effect of the elimination of the spuriousity in the E20 excitations, which are connected also with the number of particle spuriousity, is analyzed in the top panels of the Fig.6. In the case of the isoscalar E20 strength function (left top panel with $\mu = 0$) the black solid curve coincides with the red dotted one and it means that the spuriousity in the E20 RPA isoscalar excitations is negligible. The small lowest energy peak in the isovector E20 strength function (right top $\mu = 0$ panel in the Fig.6) is fully eliminated by our approach. The E21 spuriousity for the case $\mu = 1$ is connected with the rotational invariance of the intrinsic Hamiltonian and it is discussed in the next subsection. In the case of the quadrupole E22 excitations with $\mu = 2$ there is no any spurious mode.

C. Elimination of the spuriousity from E21 and M11 excitations

E21 and M11 excitations correspond to the angular momentum projection $\mu = \pm 1$ and parity $\pi = +1$. The spuriousity in this case is connected with the violation of the symmetry of the intrinsic Hamiltonian with respect to the rotation round the axis perpendicular to the symmetry axis of the nucleus. If the z-th axis of the intrinsic frame coincides with the nucleus symmetry axis then, without losing the generality, the x-th and y-th intrinsic axes can be chosen in such a way that the rotation spuriousity elimination is connected with the following requirement,

$$[\hat{H}_{intr}, \hat{J}_{\mu=1}] = 0 \quad (85)$$

where $\hat{J}_1 = -\frac{1}{\sqrt{2}}(\hat{J}_x + i\hat{J}_y)$ is the operator of the $\mu = 1$ component of the the 1-st rank tensor constructed from the intrinsic x- and y- components of the total angular momentum operator, which consists from the orbital and

spin parts,

$$\hat{J}_1 = \hat{L}_1 + \frac{1}{2}\sigma_{+1} = \frac{-\hat{L}_x - i\hat{L}_y}{\sqrt{2}} + \frac{1}{\sqrt{2}} \begin{pmatrix} 0 & -1 \\ 0 & 0 \end{pmatrix} \quad (86)$$

where $\sigma_{+1} \equiv -\frac{1}{\sqrt{2}}(\sigma_x + i\sigma_y)$ with σ_x and σ_y Pauli matrices acting in the spin space of the single-particle wave functions. Since the operator \hat{J}_1 is time-odd then, supposing (85), \hat{J}_1 can be identified with the generalized linear momentum operator \hat{P}_0 of the zero energy mode for the RPA solution with $\mu^\pi = 1^+$. Then the two-quasiparticle part of the operator \hat{J}_1 (that means the part expressed in the language of quasiparticle creation and annihilation operators by means of terms of $\alpha^+\alpha^-$ or $\alpha\alpha^-$ type) is

$$\hat{P}_0 \equiv \hat{J}_1 \approx \sum_{ij} \mathcal{P}_{ij}^{(0)} (\alpha_i^+ \alpha_j^+ - \alpha_j^- \alpha_i^-) \quad (87)$$

where $\mathcal{P}_{ij}^{(0)} = \langle ij | \hat{J}_1 | 0 \rangle$ are real two-quasiparticle matrix elements. The imaginary two-quasiparticle matrix elements $\Theta_{ij} = \mathcal{X}_{ij}^{(0)} = \langle ij | \hat{X}_0 | 0 \rangle$ of the corresponding angle $\hat{\Theta}$ conjugated to \hat{J}_1 ($[\hat{X}_0, \hat{P}_0^\dagger] = [\hat{\Theta}, \hat{J}_1^\dagger] = i\hbar$),

$$\hat{\Theta} \equiv \hat{X}_0 = \sum_{ij} \mathcal{X}_{ij}^{(0)} (\alpha_i^+ \alpha_j^+ + \alpha_j^- \alpha_i^-) \quad (88)$$

is given by the inversion (34) where the effective spurious mass M_0 , calculated by combining (34) with (13) for $\nu = 0$, has physical meaning of the principal $\mu = 1$ component of the moment of inertia \mathcal{F}_1 ,

$$M_0 = \mathcal{F}_1 \approx 2 \sum_{ij,kl=1}^N J_{ij}^{(\mu=1)*} (A - B)_{ij,kl}^{-1} J_{kl}^{(\mu=1)} \quad (89)$$

If we neglect residual interaction in matrices A and B (see (6)) then the expression (89) corresponds to the well-known Belyaev formula [38] for the moment of inertia \mathcal{F} . In this paper matrices A and B are calculated using (6) with the Skyrme BCS field with corresponding Skyrme residual interaction. Using known two-quasiparticle matrix amplitudes $\mathcal{X}_{ij}^{(0)}$ and $\mathcal{P}_{ij}^{(0)}$ all physical free of spuriousity states $|\nu'\rangle$ are then determined by (23) with corresponding matrix elements (28) for $\hat{T} \equiv \hat{\mathcal{M}}_{E21}(\Delta T)$ (see (40)) and $\hat{T} \equiv \hat{\mathcal{M}}_{M11}(\Delta T)$ (see (44)) for E2 and M1 transition operators.

In the Fig.6 the spurious elimination effect is demonstrated for isoscalar $\Delta T = 0$ (left panels) and isovector $\Delta T = 1$ (right panels) E2 μ ($\mu = 0, \pm 1, \pm 2$) strength functions. Similarly as in previous figures the black solid curves correspond to the calculations involving spuriousity elimination corrections and red dotted curves are connected with calculations without any spuriousity elimination corrections. As it was discussed in the previous subsection E20 ($\mu = 0$) strength functions (top panels with $\mu = 0$) are connected with the number of particle while the elimination of the spuriousity in E21 transitions ($\mu = 1$ panels) is linked with the requirement of

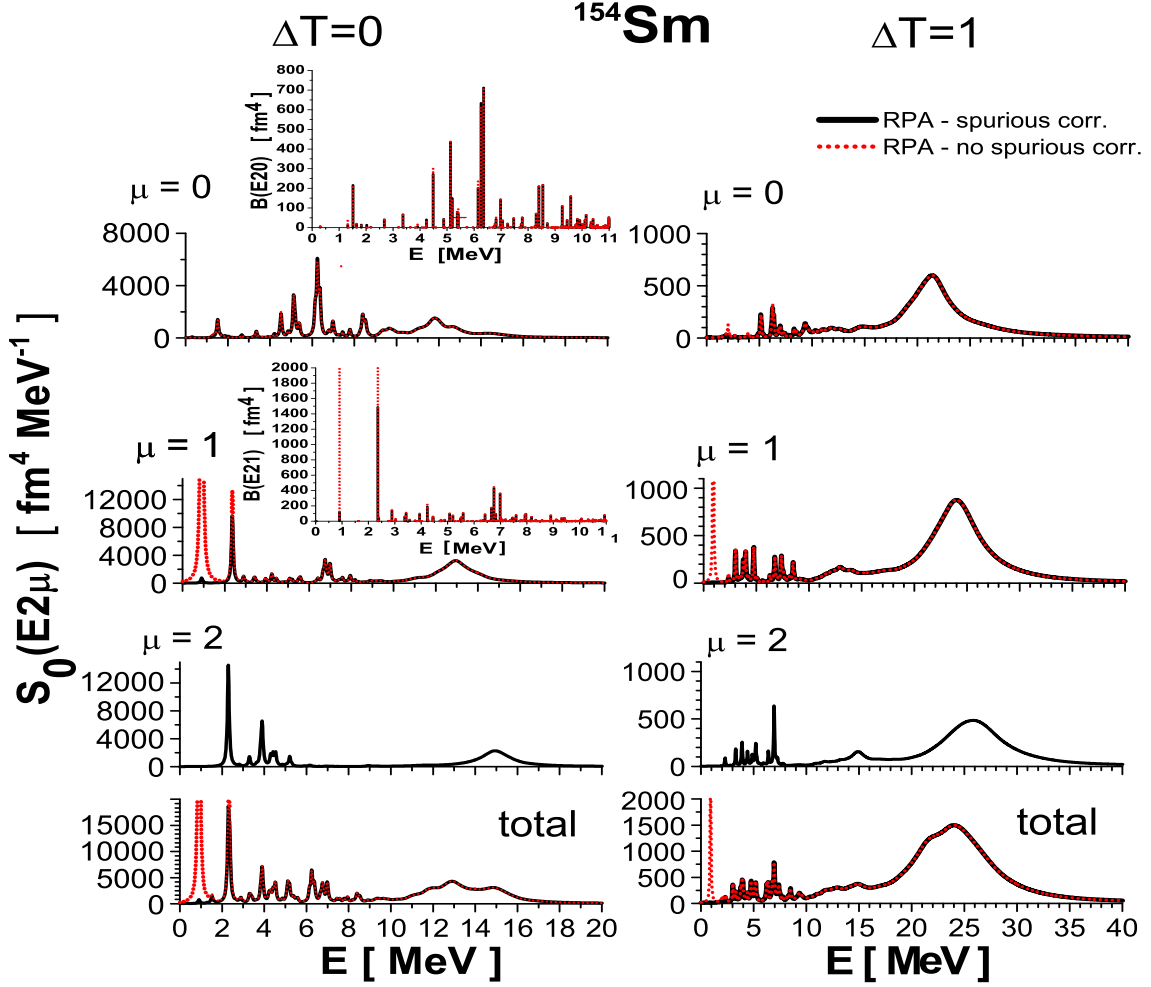


FIG. 6: Isoscalar (left panels) and isovector (right panels) strength functions of electric quadrupole E2 excitations, calculated by means of (49), are shown. The top panels correspond to $\mu^\pi = 0^+$, middle panels to $\mu^\pi = \pm 1^+$ and $\mu^\pi = \pm 2^+$ angular momentum projections, and the bottom panels demonstrate the total (summed over all projections μ) strength functions $S_0(E2\mu; \Delta T = 0, 1; E)$. Red dotted curves were obtained by the calculation without the spuriocity corrections and black solid lines involve the spuriocity-elimination corrections. Insets in two panels for $\Delta T = 0$ transitions for $\mu = 0$ and $\mu = 1$ show the reduced probability of excitation of lowest states with energies up to 11 MeV calculated with (black columns) and without (dashed red columns) spuriocity elimination corrections.

the validity of (85). The E22 strength functions ($\mu = 2$ panels) are free of the spuriocity because there is no any operator (generator) with the selection rule corresponding to $\mu^\pi = 2^+$ which would commute to zero with the intrinsic Hamiltonian. Therefore there is no red dotted curves in the $\mu = 2$ panels in the Fig.6. In the bottom panels (marked as "total") the total strength function $\sum_{\mu=0,\pm 1,\pm 2} S_0(E2\mu; \Delta T; E)$ for $\Delta T = 0$ and $\Delta T = 1$ is shown. One can see that our spuriocity elimination method reduces the spuriocity peak to the minimum and in the comparison with E0 and E1 transitions the spuriocity admixtures in RPA solutions with nonzero energies are very small in all $\Delta T = 0, 1$ cases.

In order to demonstrate how our method for the elimination of the rotation type spuriocity works in the Fig.7 the projection of the nucleon transition current

$\delta \vec{j}_{s; \Delta T=0}(\vec{r})$ on the x-z plane of the intrinsic frame is shown. According to the Fig.6 the first RPA solution for $\mu^\pi = 1^+$, with the energy 0.95 MeV, corresponds to the spurious mode (because the red dotted peak for $\mu = 1$ and for both $\Delta T = 0$ and $\Delta T = 1$ with the energy 0.95 MeV is eliminated by our spuriocity elimination approach). In the panel (a) of the Fig.7 the transition current projection $\delta \vec{j}_{\nu=1; \Delta T=0}(\vec{r}) = \langle 0 | Q_{\nu=1}, \hat{j}_{nuc}(\vec{r}) | 0 \rangle$ for uncorrected RPA solution $|s\rangle = |\nu=1\rangle = Q_{\nu=1}^\dagger |0\rangle$ with the energy 0.95 MeV is demonstrated. One can see a clear rotation character of the nucleon flow. In the panel (b) the projection on the x-z plane of the correction spurious transition current $\delta \vec{j}_{sp\ corr}(\vec{r})$ given by the second term of (32) (with $\hat{T} = \hat{j}_{nuc}(\vec{r})$, $\hat{P}_0 = \hat{J}_1$ and $\hat{X}_0 = \hat{\Theta}$) is shown. In the panel (c) there is the projection on x-z plane of the

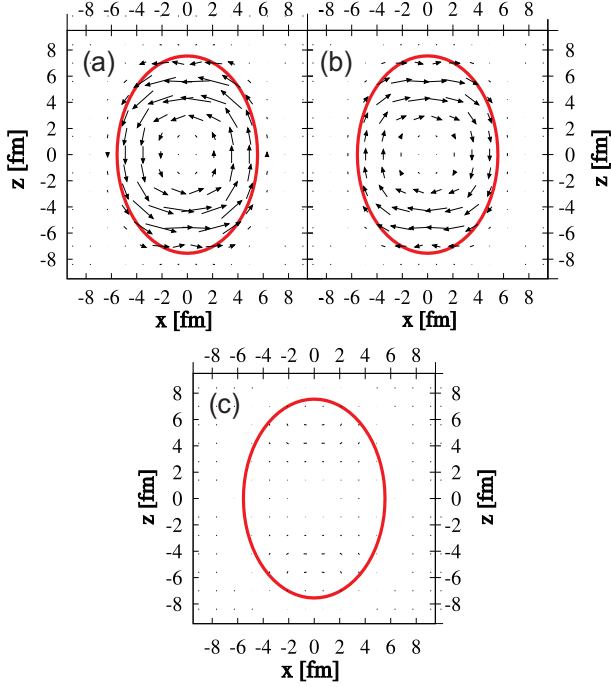


FIG. 7: The convection transition current $\delta j_{conv}(\vec{r})$ in the x - z plane of the intrinsic frame are demonstrated for the first (spurious) RPA solution for $\mu^\pi = 1^+$ with the energy $\hbar\omega_{\nu=1} = 0.95$ MeV. The panel (a) shows the projection of the transition current $\delta j_{\nu=1; \Delta T=0}(\vec{r})$ without any spuriousity elimination corrections. In the panel (b) there is the spuriousity-correction transition current $\delta \vec{j}_{sp\ corr}(\vec{r})$ given by the second term in (29). The total corrected transition current $\delta j_{\nu'=1; \Delta T=0}(\vec{r})$ (see (90)) is shown in the panel (c).

total (corrected) transition current $\delta j_{\nu'; \Delta T=0}(\vec{r})$ given as the sum of uncorrected $\delta j_{\nu=1; \Delta T=0}(\vec{r})$ and the correction $\delta \vec{j}_{sp\ corr}(\vec{r})$,

$$\delta j_{\nu'=1; \Delta T=0}(\vec{r}) = \delta j_{\nu=1; \Delta T=0}(\vec{r}) + \delta \vec{j}_{sp\ corr}(\vec{r}) \quad (90)$$

which is practically zero. The correction term $\delta \vec{j}_{sp\ corr}(\vec{r})$ cancels fully the transition current $\delta j_{\nu=1; \Delta T=0}(\vec{r})$ of the first (spurious) solution of the RPA equation. Similar effect can be seen for the isovector transition current of the first RPA solution with the energy 0.95 MeV.

Fig.8 shows the spuriousity elimination effect in the M1 excitations in ^{154}Sm . The M1 transition operator (44) consists from the orbital part (the first term in (44)) and spin part (the second term in (44)). It is necessary to remind that the orbital part of the operator $\hat{M}_{M1\mu}(\Delta T)$ is responsible for the excitation of so called scissor modes and spin part for spin-flip M1 modes.

The top part of the Fig.8 illustrates the M10 strength function for $\Delta T = nat$ excitations for $\mu^\pi = 0^+$. This multipolarity is connected with the number-of-particles operator discussed in the subsection III.B. However, due to inherent separation of electric and magnetic subspaces

for $\mu = 0$ (we take advantage of it by symmetrization/antisymmetrization of densities and currents), the corresponding spurious state ends up in electric subspace and M10 is not affected. Just for the demonstration of the fact that in the case of $\mu = 0$ there is no direct excitation of the scissor modes, in the top $\mu = 0$ graph in the Fig.8 the contributions of the orbital (green dashed curve) and spin (the blue dotted curve) parts of the M10 transition operator to the total strength function $S_0(M10, \Delta T = nat; E)$ are shown. By other words it means that for $\mu = 0$ the total M1 strength is given only by the spin M10 transition operator.

In the lower part of the Fig.8 the $\mu = 1$ part of the M1 strength function is presented (concretely the total M11 strength, orbital part of the M11 strength, and the spin part of the M11 strength). The spuriousity in the case of $\mu = 1$ is linked with the spurious nuclear rotation in the intrinsic frame and it concerns only orbital part of the $M1, \pm 1$ strength. Our method of the spuriousity elimination reduces the spurious peak seen at the energy 0.95 MeV in the orbital M11 strength function practically to zero.

In the end of the subsection dealing with the elimination of the rotation spuriousity generated by the operator \hat{J}_1 of the $\mu = 1$ component of the total angular momentum we can compare the value of the moment of inertia $\mathcal{F}_1^{(th)}$ calculated by means of (89) with the experimental value $\mathcal{F}_1^{(exp)}$ extracted from the experimental energy of the first 2_1^+ level of the ground state rotational band according to the relation $\mathcal{F}_1^{(exp)} = 3\hbar^2 / E_{2_1^+}$; $\mathcal{F}_1^{(exp)} = 37\hbar^2 / \text{MeV}$ and our calculations give $\mathcal{F}_1^{(th)} = 57\hbar^2 / \text{MeV}$. The discrepancy can be ascribed to the neglecting of the complex configurations and the finiteness of the used configuration space.

IV. CONCLUSION

A general simple method for elimination of spurious admixtures (SA) from RPA/QRPA intrinsic nuclear excitations is proposed. The most relevant cases are illustrated by Skyrme QRPA calculations for axially deformed ^{154}Sm . They include violation of the translational invariance (isovector E1 and isoscalar toroidal and compression E1 excitations), rotational invariance (E2(K=1) excitations), and pairing-induced non-conservation of the particle number (E2(K=0) and E0 excitations). High efficiency and accuracy of the method were demonstrated. The method reproduces familiar effective charges and corrections which are already widely used for SA elimination. For axial deformed nuclei, additional deformation-induced corrections are suggested.

The method is universal. It can be applied to various self-consistent RPA/QRPA approaches. Both spherical and deformed nuclei can be covered. The refinement can be done for RPA/QRPA states and directly for various electric and magnetic responses. The main advantage of

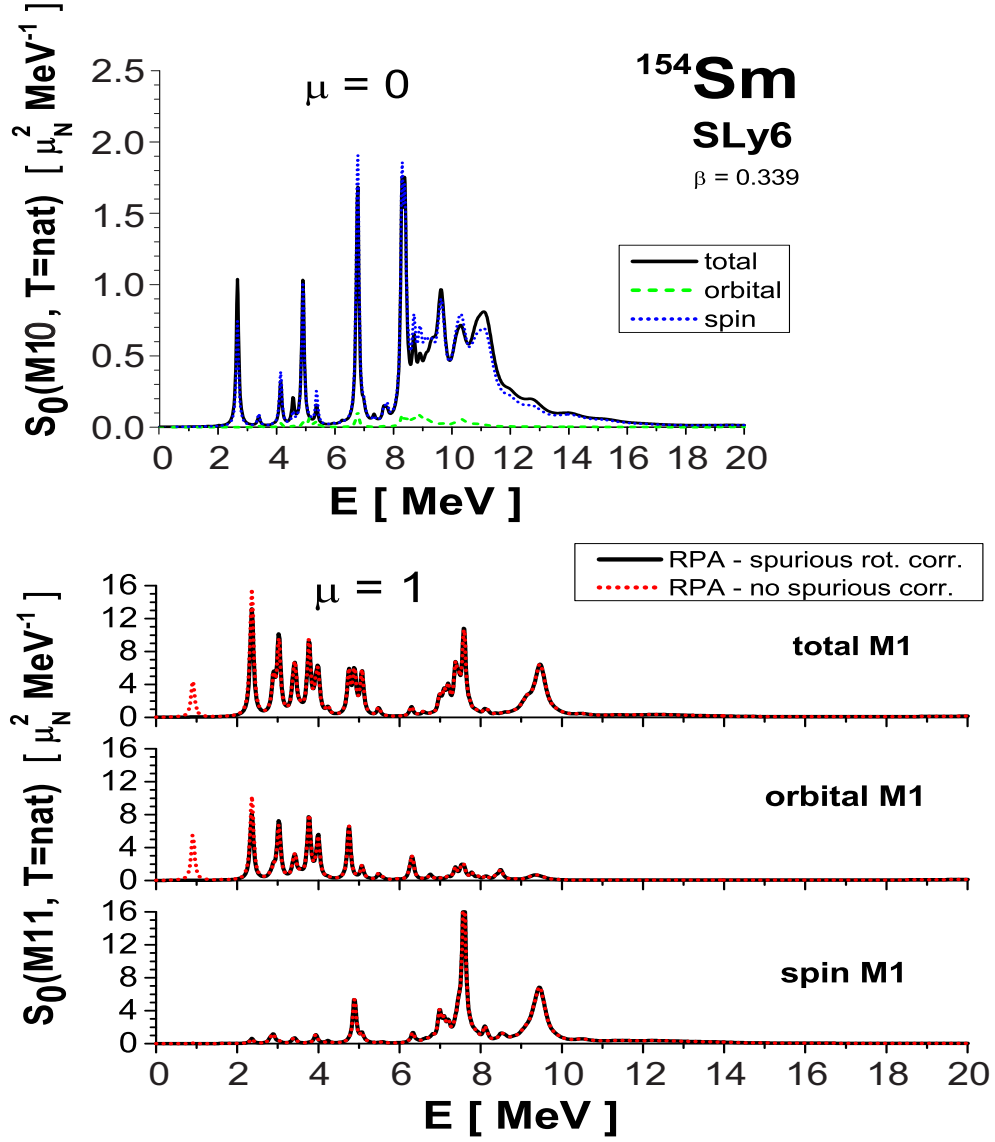


FIG. 8: Strength function of the M10 excitations is demonstrated in the top part of the figure and the strength function of the M11 excitations is shown in the bottom part, where the total M11 strength (its transition operator involves both terms of (44)), orbital M11 strength (transition operator involves only the first term of (44)), and spin M11 strength (transition operator involves only the second term of (44)) are depicted in separate plots.

the method is that it considers various SA corrections on the same theoretical ground, using the basic RPA features.

from Slovak Research and Development Agency under Contract No. APVV-15-0225.

The work was partly supported by Votruba-Blokhincev (Czech Republic-BLTP JINR) and Heisenberg-Landau (Germany - BLTP JINR) grants. The support of the Czech Science Foundation Grant Agency (project P203-13-07117S) is appreciated. A.R. is grateful for support

Appendix A: Basic transformations

Appendix A: Cylindrical coordinate expressions for the operator $f(r) Y_{\lambda\mu}(\hat{r})$

We are listing cylindrical coordinate ($\vec{r} \equiv (\varrho, z, \phi)$) expressions for dipole $\lambda = 1$ and quadrupole $\lambda = 2$ operators $f(r) Y_{\lambda\mu}(\hat{r})$ for arbitrary radial function $f(r)$, where generally we have

$$f(r) Y_{\lambda\mu}(\hat{r}) = f_{\lambda\mu}(\varrho, z) e^{i\mu\phi} \quad (\text{A1})$$

with $f_{\lambda-\mu}(\varrho, z) = (-1)^\mu f_{\lambda\mu}(\varrho, z)$.

For the case of $\lambda = 1$, we have

$$\begin{aligned} f(r) Y_{10}(\hat{r}) &= \sqrt{\frac{3}{4\pi}} \frac{z}{r} f(r) = f_{10}(\varrho, z) \\ f(r) Y_{11}(\hat{r}) &= -\sqrt{\frac{3}{8\pi}} \frac{x+iy}{r} f(r) = f_{11}(\varrho, z) e^{i\phi} \\ f(r) Y_{1-1}(\hat{r}) &= \sqrt{\frac{3}{8\pi}} \frac{x-iy}{r} f(r) = f_{1-1}(\varrho, z) e^{-i\phi} \end{aligned} \quad (\text{A2})$$

where

$$\begin{aligned} f_{10}(\varrho, z) &= \sqrt{\frac{3}{4\pi}} \frac{z}{\sqrt{\varrho^2 + z^2}} f(r = \sqrt{\varrho^2 + z^2}) \\ f_{11}(\varrho, z) &= -\sqrt{\frac{3}{8\pi}} \frac{\varrho}{\sqrt{\varrho^2 + z^2}} f(r = \sqrt{\varrho^2 + z^2}) \\ f_{1-1}(\varrho, z) &= \sqrt{\frac{3}{8\pi}} \frac{\varrho}{\sqrt{\varrho^2 + z^2}} f(r = \sqrt{\varrho^2 + z^2}) \end{aligned} \quad (\text{A3})$$

For the case $\lambda = 2$, we have

$$\begin{aligned} f(r) Y_{20}(\hat{r}) &= \sqrt{\frac{5}{16\pi}} \frac{2z^2 - x^2 - y^2}{r^2} f(r) = f_{20}(\varrho, z) \\ f(r) Y_{21}(\hat{r}) &= -\sqrt{\frac{15}{8\pi}} \frac{z(x+iy)}{r^2} f(r) = f_{21}(\varrho, z) e^{i\phi} \\ f(r) Y_{2-1}(\hat{r}) &= \sqrt{\frac{15}{8\pi}} \frac{z(x-iy)}{r^2} f(r) = f_{2-1}(\varrho, z) e^{-i\phi} \\ f(r) Y_{22}(\hat{r}) &= \sqrt{\frac{15}{32\pi}} \frac{x^2 - y^2 + 2ixy}{r^2} f(r) = \\ &= f_{22}(\varrho, z) e^{2i\phi} \\ f(r) Y_{2-2}(\hat{r}) &= \sqrt{\frac{15}{32\pi}} \frac{x^2 - y^2 - 2ixy}{r^2} f(r) = \\ &= f_{2-2}(\varrho, z) e^{-2i\phi} \end{aligned} \quad (\text{A4})$$

where

$$\begin{aligned} f_{20}(\varrho, z) &= \sqrt{\frac{5}{16\pi}} \frac{2\varrho^2 - z^2}{\varrho^2 + z^2} f(r = \sqrt{\varrho^2 + z^2}) \\ f_{21}(\varrho, z) &= -\sqrt{\frac{15}{8\pi}} \frac{z\varrho}{\varrho^2 + z^2} f(r = \sqrt{\varrho^2 + z^2}) \\ f_{2-1}(\varrho, z) &= \sqrt{\frac{15}{8\pi}} \frac{z\varrho}{\varrho^2 + z^2} f(r = \sqrt{\varrho^2 + z^2}) \\ f_{22}(\varrho, z) &= \sqrt{\frac{15}{32\pi}} \frac{\varrho^2}{\varrho^2 + z^2} f(r = \sqrt{\varrho^2 + z^2}) \\ f_{2-2}(\varrho, z) &= \sqrt{\frac{15}{32\pi}} \frac{\varrho^2}{\varrho^2 + z^2} f(r = \sqrt{\varrho^2 + z^2}) \end{aligned} \quad (\text{A5})$$

-
- [1] D.J. Row, *Nuclear Collective Motion* (Mothuen, London, 1970).
- [2] E.R. Marshalek and J. Weneser, *Ann. Phys. (NY)*, **53**, 569 (1969).
- [3] P. Ring and P. Schuck, *Nuclear Many Body Problem*, (Springer-Verlag N.Y.-Hedelberg-Berlin, 1980).
- [4] J.P. Blaizot and G. Ripka, *Quantum Theory of Finite Systems*, Ch. 10 (MIT Press, Cambridge, MA, 1986).
- [5] M. Bender, P.-H. Heenen, and P.-G. Reinhard, *Rev. Mod. Phys.* **75**, 121 (2003).
- [6] T. Nikšić, D. Vretenar, and P. Ring, *Phys. Rev. C* **74**, 064309 (2006).
- [7] N. Van Giai and H. Sagawa, *Nucl. Phys.A* **371**, 1 (1981).
- [8] M.N. Harakeh, and A. van der Woude, *Giant Resonances*, (Clarendon Press Oxford, 2001).
- [9] J. Kvasil, V.O. Nesterenko, W. Kleinig, P.G. Reinhard, and P. Vesely, *Phys. Rev. C* **84**, 034303 (2011).
- [10] G. Colo, N. Van Giai, P.F. Bortignon, and M.R. Qualia, *Phys. Lett.* **B485**, 362 (2000).
- [11] Jun Li, G. Colo, and J. Meng, *Phys. Rev. C* **78**, 064302 (2008).
- [12] T. R. Rodríguez and J. L. Egido, *Phys. Rev. Lett.* **99**, 062501 (2007).
- [13] N.N. Arsenyev and A.P. Sereryukhin, *Phys. Part. Nucl. Lett.* **7**, 112 (2010).
- [14] L.M. Robledo, T.R. Rodríguez, R.R. Rodríguez-Guzmán, arXiv:1807.02518v1[nucl-th].
- [15] D. Vretenar, A. V. Afanasjev, G. A. Lalazissis, and P. Ring, *Phys. Rep.* **409**, 101 (2005).
- [16] N. Paar, D. Vretenar, E. Khan, and G. Colo, *Rep. Prog. Phys.* **70**, 691 (2007).
- [17] W. Kleinig, V.O. Nesterenko, J. Kvasil, P.-G. Reinhard and P. Vesely, *Phys. Rev. C* **78**, 044313 (2008).
- [18] J. Kvasil, V.O. Nesterenko, A. Repko, W. Kleinig, and P.-G. Reinhard, *Phys. Rev. C* **94**, 064302 (2016).
- [19] J. Terasaki, J. Engel, M. Bender, J. Dobaczewski, W. Nazarewicz, M. Stoitsov, *Phys. Rev. C* **82**, 034326 (2010).
- [20] V.O. Nesterenko, V. G. Kartavenko, W. Kleinig, R.V. Jolos, J. Kvasil, and P.-G. Reinhard, *Phys. Rev. C* **93**, 034301 (2016).
- [21] D.J. Thouless, *Nucl. Phys.* **22**, 225 (1960).
- [22] D.J. Thouless and J.G. Valatin, *Nucl. Phys.* **31**, 211 (1962).
- [23] H. Nakada, *Prog. Theor. Exp. Phys.* **2017**, 023D03.
- [24] N.I. Pyatov and D.I. Salamov, *Nucleonika* **22**, 127 (1977).
- [25] F. Palumbo, *Nuclear Physics* **99**, 100 (1967).

- [26] F. Doenau, Phys. Rev. Lett. **94**, 092503 (2005).
- [27] P.-G. Reinhard, Ann. Phys. (Leipzig) **1**, 632 (1992).
- [28] V.O. Nesterenko, J. Kvasil, and P.-G. Reinhard, Phys. Rev. C **66**, 044307 (2002).
- [29] V.O. Nesterenko, W. Kleinig, J. Kvasil, P. Vesely, P.-G. Reinhard, and D. S. Dolci, Phys. Rev. C **74**, 064306 (2006).
- [30] D. A. Varshalovich, A. N. Moskalev, and V. K. Khersonskii, *Quantum Theory of Angular Momentum* (World Scientific, Singapore, 1976).
- [31] R. Alacron, R.M. Laszewski, D.S. Dale, Phys. Rev. **C40**, R1097 (1989).
- [32] J. Kvasil, V.O. Nesterenko, W. Kleinig, D. Bozik, P.-G. Reinhard, N. Lo Iudice, Eur. Phys. J. **A49**, 119 (2013).
- [33] E. Chabanat, P. Bonche, P. Haensel, J. Meyer, R. Schaeffer, Nucl. Phys. **A635**, 231 (1998).
- [34] A. Repko, *Theoretical description of nuclear collective excitations*, PhD thesis, Math.-Phys. Faculty of Charles University in Prague (2015), arXiv:1603.04383 [nucl-th].
- [35] G.M. Gurevich, L.E. Lazareva, V.M. Mazur, S.Yu Merkulov, G.V. Solodukov, and V.A. Tyutin, Nucl. Phys. **A351**, 257 (1981).
- [36] D.H. Youngblood, Y.W. Lui, H.L. Clark, B. John, Y. Tokimoto, and X. Chen, Phys. Rev. **C69**, 034315 (2004).
- [37] M. Itoh, et al, Phys. Rev. **C68**, 064602 (2003).
- [38] S.T. Belyaev, Nuclear Physics **64**, 17 (1961).